1

Transport of Gases and Vapors in Glassy and Rubbery Polymers

Scott Matteucci, Yuri Yampolskii, Benny D. Freeman and Ingo Pinnau

COPYRIGHTED MATERIAL

1.1 Background and Phenomenology

Transport in non-porous polymeric membranes is based on the so-called 'solution–diffusion' concept [1,2]. This model, formulated in the 19th century, is grounded in the works of J. K. Mitchell [3], T. Graham [4] and S. von Wroblewski [5], who demonstrated that the presence of microscopic open pores or capillaries was not a prerequisite for mass transfer through polymeric films (or septa as they were referred to), such as natural rubber. First, Graham in 1829 [4], and then Mitchell in 1831 [3], noted that gases were capable of permeating through non-porous rubber films and that this process was related to gas dissolution and diffusion in the polymeric materials. The currently accepted interpretation of such experiments was given several decades later by Graham [4] (this and other articles from the early history of membrane science have been reproduced, in part, in a special issue of the *Journal of Membrane Science*) [6]. Because he did not find a monotonic correlation between the rates of transport and the known gas phase diffusion coefficients of the penetrant molecules, Graham concluded that the process of permeation comprised two stages: sorption of gas by the rubber 'that must depend upon a kind of chemical affinity' and diffusion of the sorbed gas molecules [4]. The sorbed gas, as he wrote, 'comes to evaporate .... and reappears as gas on the other side of the membrane. Such evaporation is the same into vacuum and into another gas, being equally gas-diffusion in both circumstances' [4].

Empirical observations of the pressure and thickness dependence of the steady-state gas permeation rate or flux, N, led von Wroblewski [5] to propose the following relation:

$$N = P(\Delta p/l) \tag{1.1}$$

where Δp is the pressure difference across the membrane, and l is its thickness. The proportional coefficient in this equation, P, was defined as the permeability coefficient. While permeability defines gas transport as an intrinsic physical property for a given polymer/gas pair, this expression does not reveal the molecular basis of permeation.

A more fundamental basis for permeation may be derived by considering a plane polymer film of thickness l separating two regions filled with a single gas, as shown in Figure 1.1. The gas pressure on the upstream (or high-pressure) side of the film is p_2, while the gas pressure on the downstream (or low-pressure) side is p_1. At steady-state, the gas flux at any point inside the polymer is given by Fick's first law [7]:

$$N = \left(\frac{-D_{\text{loc}}}{1-w}\right)\left(\frac{\mathrm{d}C}{\mathrm{d}x}\right) \tag{1.2}$$

where N is the gas flux relative to fixed coordinates, C is the gas concentration, x is the distance across the film, w is the mass fraction of gas in the polymer, and D_{loc} is the binary mutual diffusion

Materials Science of Membranes for Gas and Vapor Separation Edited by Yu. Yampolskii, I. Pinnau and B. D. Freeman
© 2006 John Wiley & Sons, Ltd

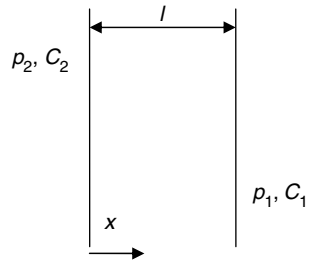


Figure 1.1 Representation of gas or vapor transport through a non-porous polymeric membrane; p_2 is presumed to be greater than p_1

coefficient of the gas in the polymer. Integration across the film (from $x = 0$ to $x = l$) yields:

$$N = \frac{1}{l}\int_{C_1}^{C_2} \frac{D_{\text{loc}}}{1-w}\,\mathrm{d}C \tag{1.3}$$

where C_1 and C_2 are the gas concentrations in the polymer at the downstream and upstream faces of the membrane, respectively, which are in equilibrium with the external pressures p_1 and p_2, respectively. This relationship can be written as follows:

$$N = \frac{C_2 - C_1}{l} D \tag{1.4}$$

where D, the average effective diffusion coefficient, is defined as:

$$D = \frac{1}{C_2 - C_1}\int_{C_1}^{C_2} \frac{D_{\text{loc}}}{1-w}\,\mathrm{d}C \tag{1.5}$$

With this definition, the permeability of a gas in a polymer can be expressed as:

$$P = \frac{Nl}{p_2 - p_1} = \left(\frac{C_2 - C_1}{p_2 - p_1}\right) D \tag{1.6}$$

Equation (1.6) is derived for 'pure-gas' permeation. To extend the definition to mixtures, the total pressures p_2 and p_1 should be replaced with the corresponding partial pressures of the component of interest on the upstream and downstream sides of the membrane, respectively. To account for the effects of gas-phase non-idealities on the driving force for permeation, the pressures (or partial pressures, in the case of mixtures) are typically replaced by fugacities (e.g. with high-pressure CO_2 feed streams) [8].

When the upstream pressure and concentration (p_2 and C_2, respectively) are much greater than their downstream analogs, this result simplifies as follows:

$$P = \frac{C_2}{p_2} D \tag{1.7}$$

The equilibrium solubility coefficient of a gas in a polymer is the ratio of the concentration of gas dissolved in the polymer at equilibrium to the pressure of gas (or partial pressure in the case of mixtures) in the contiguous gas phase [7]:

$$S = C/p \tag{1.8}$$

When this result is applied to Equation (1.7), one obtains:

$$P = DS \tag{1.9}$$

where the solubility coefficient, S, is evaluated at the upstream face of the membrane (i.e. $S = C_2/p_2$). From this result, P depends upon two factors: (1) a thermodynamic term, S, characterizing the number of gas molecules sorbed into and onto the polymer and (2) a kinetic or mobility term, D, characterizing the mobility of gas molecules as they diffuse through the polymer. In other words, permeability, which is the pressure- and thickness-normalized gas flux through the polymer film (cf. Equation (1.1)), depends upon the product of the number of gas molecules that dissolve in the polymer and their rate of migration through the polymer matrix. Equation (1.9) emphasizes that high permeability coefficients can result from large D values, large S values, or both. For example, some so-called 'fast' (i.e. high-permeability) gases display (i) large diffusion coefficients (e.g. He or H_2), (ii) high solubility coefficients (e.g. CO_2) or (iii) both (e.g. H_2O).

Many different experimental strategies are used to determine the P, D, and S values in polymers, and these methods have been thoroughly reviewed [9,10]. A common technique involves measuring permeability in a steady-state gas permeation experiment and D in the transient regime that precedes the attainment of steady-state in a permeation experiment, which is the so-called time-lag method [11]. S is then estimated (using the solution–diffusion model) as the ratio of P divided by D. A more accurate procedure relies

on independent determinations of P in steady-state permeation experiments and S in equilibrium-sorption measurements [12–14]. In this case, D is estimated, using the solution–diffusion model (i.e. Equation (1.9)), as the ratio of P divided by S. The third possible alternative – direct measurement of S and D in kinetic sorption experiments and estimating P as the product of S and D – is not used very often [14]. In any event, it is extremely rare to independently determine S, D, and P for mass transport in polymers, underscoring the popularity of the solution–diffusion mode. A more thorough review and in-depth discussion of this model is presented in the chapter by Wijmans and Baker. This topic has also been the subject of several articles [2,15].

In the SI system, permeability coefficients are expressed in the following units:

$$P = \text{mol} \cdot (\text{m}^2\,\text{s}\,\text{Pa}) \tag{1.10}$$

However, a more widely used and accepted unit for P is:

$$1\,\text{barrer} = 10^{-10}\,\text{cm}^3(\text{STP})\text{cm}/(\text{cm}^2\,\text{s}\,\text{cm}\,\text{Hg})$$

Permeability coefficients of common gases in polymers span a range of more than seven orders of magnitude, from 10^{-3} to 10^4 barrer or more.

Commercial gas separation membranes differ significantly in their morphology from that of the thick, isotropic dense polymer films considered above. A typical integral-asymmetric or thin-film composite membrane has a thin selective layer (often in the range of 200 Å to 1 μm) supported by a microporous layer [16,17]. Ideally, the microporous layer provides mechanical support for the thin selective layer, which is the dominant mass-transfer resistance of the entire structure. Often, the thickness of the selective layer is difficult or impossible to measure because, in commercial gas separation membranes based on glassy polymers, there is often very little chemical contrast between the selective layer and the support layer. Furthermore, the selective layer is often estimated to be of the order of 50 to 100 nm in thickness (and, in some cases, perhaps less), making it difficult to image. In such cases, pressure-normalized steady-state flux, or permeance (Q or P/l), is used to characterize the gas transport rate through such separating membranes. The accepted units for Q are: mol/(m^2 s Pa) (SI), m^3 (STP)/(m^2 h atm) or cm^3(STP)/(cm^2 s (cm Hg)). Permeance is also expressed in Gas Permeation Units (GPU), where 1 GPU $= 10^{-6}$ cm^3(STP)/(cm^2 s (cm Hg)). A permeance of 1 GPU corresponds to a membrane exhibiting an intrinsic permeability of 1 barrer and having a selective layer thickness of 1 μm.

Another key characteristic of gas separation membranes is their selectivity. The ideal selectivity is defined as follows [7]:

$$\alpha_{AB} = P_A/P_B \tag{1.11}$$

where P_A and P_B are the permeability coefficients of gases A and B, respectively. Commonly, the more permeable gas is taken as A, so that $\alpha_{A/B} > 1$. Bearing in mind Equation (1.9), the ideal selectivity can be partitioned into diffusivity and solubility selectivity as follows:

$$\alpha_{AB} = (D_A/D_B)(S_A/S_B) = \alpha_{AB}^{D}\alpha_{AB}^{S} \tag{1.12}$$

where S_i and D_i are the solubility and diffusion coefficients of species i, respectively. The independent analysis of α_{AB}^{D} and α_{AB}^{S} is very helpful in rationalizing gas separation properties in polymers. The ideal separation factor can also be determined from pure-gas permeance values as follows:

$$\alpha_{AB} = \frac{Q_A}{Q_B} \tag{1.13}$$

The magnitudes of α_{AB} depend sensitively on the gas pair under consideration. For example, for air separation, the values of α_{O_2/N_2} vary from approximately 2 to 15 in polymers [18]. In contrast, α_{H_2/CH_4} values range from 5 to 1000 or more [18].

When gas mixtures permeate across a membrane, the presence of one gas can, in some circumstances, influence the transport of other gases in the membrane; this phenomenon will be discussed in more detail towards the end of this chapter. In such systems, the ideal selectivity, determined from pure-gas measurements, can be a rather crude (i.e. inaccurate) measure of the 'actual' selectivity, or separation factor, of a membrane.

The separation factor, α_{AB}^{*}, determined from the ability of a membrane to separate a binary feed gas mixture, is defined as follows [7]:

$$\alpha_{AB}^{*} = (y_A/y_B)/(x_A/x_B) \tag{1.14}$$

where y_A and y_B are the mole fractions of the components produced in the permeate, and x_A and x_B are their corresponding mole fractions in the feed. The connection between α^*_{AB} and α_{AB} is provided by the following relationships, which give the mole fractions of each component produced at steady-state on the permeate (i.e. downstream) side of a membrane when the upstream side is fed with a binary mixture of gases A and B:

$$y_A = \frac{N_A}{N_A + N_B} \tag{1.15}$$

$$y_B = \frac{N_B}{N_A + N_B} \tag{1.16}$$

where N_i is the steady-state flux of component i through the membrane. Combining these expressions with the equation defining the separation factor yields:

$$\alpha^*_{AB} = \frac{N_A/N_B}{x_A/x_B} \tag{1.17}$$

The fluxes in the above expression may be related to the permeability by Equation (1.1):

$$\alpha^*_{AB} = \left(\frac{P_A}{P_B}\right)\left(\frac{p_2 x_A - p_1 y_A}{x_A}\right)\left(\frac{x_B}{p_2 x_B - p_1 y_B}\right) \tag{1.18}$$

This result may be further simplified as follows:

$$\alpha^*_{AB} = \alpha_{AB}\frac{p_2 - p_1\left(\frac{y_A}{x_A}\right)}{p_2 - p_1\left(\frac{y_B}{x_B}\right)} \tag{1.19}$$

Thus, the separation factor of a membrane depends not only on the properties of the gas–polymer system but also on process parameters such as upstream and downstream pressure, and composition [19]. When the upstream pressure is much greater than the downstream pressure, so that $p_2 \gg p_1 y_A/x_A$ and $p_2 \gg p_1 y_B/x_B$, this equation reduces to:

$$\alpha^*_{AB} = \alpha_{AB} \tag{1.20}$$

indicating that, under appropriate simplifying assumptions, the ideal selectivity is equal to the actual separation factor. In the remainder of this chapter, ideal selectivity is discussed primarily as a yardstick for characterizing membrane separation performance, since this parameter does not depend explicitly on engineering factors such as upstream/downstream pressure ratio, etc. However, ideal selectivity values determined based on pure-gas permeation properties do not necessarily capture the effects of one component in a gas mixture on the permeation properties of another component and, in some cases, (discussed later in this chapter) these effects are important.

Despite decades of systematic efforts, it has proven elusive to synthesize polymers that combine the highly desirable properties of high permeability and high selectivity. Among size-selective polymers (i.e. those that are more permeable to smaller gas molecules (e.g. H_2) than to larger gas molecules (e.g. CH_4)), there is a trade-off between permeability and selectivity, as shown in Figures 1.2(a)–1.2(c). Polymers that are more permeable tend to be less selective and vice versa. This behavior was cataloged systematically by Robeson [18], who observed empirically the existence of so-called 'upper bound lines', which define the practical upper limit of the 'clouds' of permeation data points (c.f. Figure 1.2). The upper bound lines can be predicted from rather straightforward theoretical considerations based on either free-volume or transition-state models [20,21]. For example, beginning from Equation (1.9), using concepts from Section 1.4 of this chapter on activated state diffusion and a widely used correlation of activation energy of diffusion with the square of the penetrant kinetic diameter, one can derive a relation of the following form [21]:

$$\alpha_{A/B} = \frac{\beta_{A/B}}{P_A^{\lambda_{A/B}}} \tag{1.21}$$

where P_A is the permeability of the more permeable gas (which, by convention, is always plotted on the abscissa of permeability/selectivity maps such as those presented in Figure 1.2), $\alpha_{A/B}$ is the selectivity of the more permeable (A) to the less permeable (B) gas and $\beta_{A/B}$ and $\lambda_{A/B}$ are model parameters. Most of the gas permeation data used to construct such diagrams are based on pure-gas permeation data, and so they are subject to the same cautions mentioned earlier regarding their utility in practical separations. Additionally, the data used to prepare the upper bound diagrams were in the range of ambient temperature. The slope of the upper bound lines, $\lambda_{A/B}$, can be

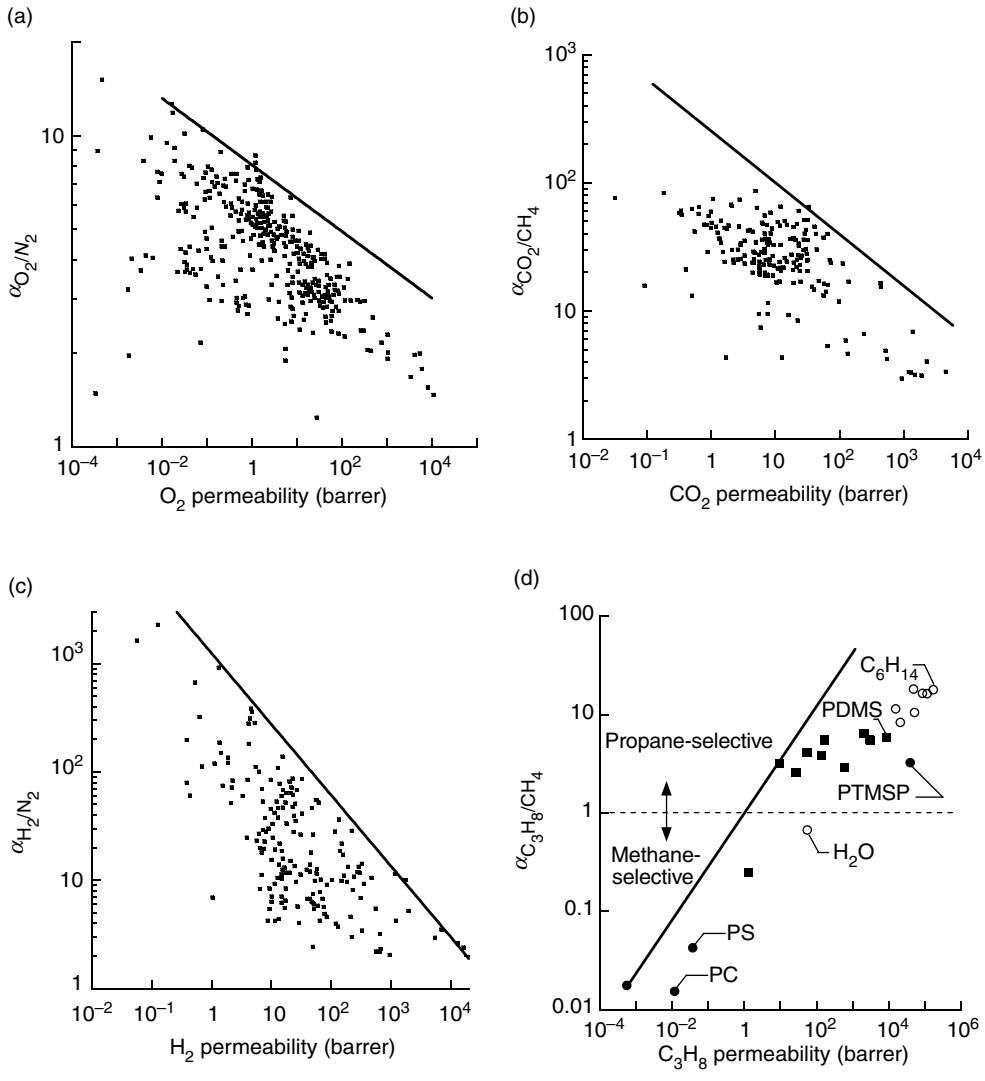


Figure 1.2 Permeability/selectivity trade-off maps for: (a) O_2/N_2; (b) CO_2/CH_4; (c) H_2/N_2; (d) C_3H_8/CH_4 [28]. For O_2/N_2, CO_2/CH_4 and H_2/N_2, the upper bound line was estimated by using the model given in Freeman [21], while for C_3H_8/CH_4, the upper bound line was drawn by eye. (a–c) Reprinted from *Journal of Membrane Science*, **62**, l. M. Robeson. 'Correlation of separation factor versus permeability for polymeric membranes', 165–185, Copyright (1991), with permission from Elsevier. (d) Reprinted from *Trends in Polymer Science*, **5**, B. D. Freeman and I. Pinnau, 'Separation of gases using solubility-selective polymers', 167–173, Copyright (1997), with permission from Elsevier

calculated to remarkable precision from the kinetic diameters of the gas molecules [21]:

$$\lambda_{A/B} = \left(\frac{d_B}{d_A}\right)^2 - 1 \qquad (1.22)$$

where d_B and d_A are the kinetic diameters of the larger and smaller gas molecules, respectively. A list of kinetic diameters of various gases is available in the literature and in Table 1.1 [22]. This result emphasizes the close connection between gas molecule size and permeation and separation properties in strongly size-sieving polymers. The position of the upper bound line, $\beta_{A/B}$, depends on gas molecule size as well

Table 1.1 Gas and vapor properties often used in correlating sorption and transport properties

Gas	Critical temperature, T_C (K)[a]	Lennard–Jones well depth, ε/k (K) [31,48]	Critical volume, V_C (cm^3/mol)[a]	Kinetic diameter, d_k (Å) [22]	Lennard–Jones diameter, d_{LJ} (Å) [48]	Chung diameter, d_C (Å)[b] [48]
He	5.2	10.2	57.5	2.6	2.551	3.123
H_2	33.2	59.7	64.9	2.89	2.827	3.251
O_2	154.6	106.7	73.5	3.46	3.467	3.389
N_2	126.2	71.4	89.3	3.64	3.798	3.616
CO	134.5	91.7	90.1	3.76	3.69	3.627
CO_2	304.2	195.2	91.9	3.3	3.941	3.651
CH_4	190.6	148.6	98.6	3.8	3.758	3.737
C_2H_6	305.3	215.7	147	—	4.443	4.27
C_2H_4	282.5	224.7	131.1	3.9	4.163	4.11
C_3H_8	369.9	237.1	200	4.3	5.118	4.731
C_3H_6	365.2	298.9	184.6	4.5	4.678	4.606
n-C_4H_{10}	425	531.4	255	4.3	4.971 [47]	5.13
i-C_4H_{10}	407.7	330.1	259	5	5.278	5.157
H_2O	647	809.1	55.9	2.65	2.641	3.093
H_2S	373.3	301.1	87.7	3.6	3.623	3.594

[a]www.NIST.gov.
[b]Chung correlation [48], where $d_C = 0.809\,V_C^{1/3}$.

as solubility:

$$\beta_{A/B} = \frac{S_A^{1+\lambda_{A/B}}}{S_B} \exp\left\{-\lambda_{A/B}\left[b - f\left(\frac{1-a}{RT}\right)\right]\right\} \tag{1.23}$$

where S_A and S_B are the solubility coefficients of the more permeable and less permeable gases, respectively. The parameters a and b are from a so-called linear free energy model, and their values are fixed for glassy polymers ($a = 0.64$, $b = 11.5$) [21]. The only adjustable constant is f, which characterizes the product of the energy barriers to open a gap to allow a penetrant to diffuse and the equilibrium interchain spacing. When f is set to 12 600 cal/mol, one achieves the best-fit to the upper bound data available in the literature [21].

From a qualitative viewpoint, the existence of permeability/selectivity trade-off relations is most easily understood from a free-volume viewpoint. The most typical way to significantly enhance the permeability of glassy polymers, such as those commonly considered as gas separation polymers, is to change the chemical structure by introducing packing-disrupting units into the polymer backbone, thereby increasing the free volume [23]. Increasing the free volume usually strongly increases the diffusion coefficients [23,24] and reduces the diffusivity selectivity, accordingly. The increase in diffusion coefficients increases permeability while the reduction in diffusivity selectivity reduces the overall permeability selectivity.

In some applications, such as the removal of higher hydrocarbons from natural gas and the removal of volatile organic compounds from air gases, it is economically desirable to use membranes that are more permeable to the larger species in the gas mixture [25–27]. Such performance can only be achieved by harnessing the much higher solubility of the larger component and selecting materials with very weak size-sieving properties, so that the diffusion selectivity, which will always favor the smaller molecule, is not so strong that the polymer is selective for the smaller molecule [28]. The permeability/selectivity map for such separations looks quite different than for the strongly size-sieving separations presented in Figures 1.2(a)–1.2(c). An example of such a reverse-selective separation, C_3H_8/CH_4, is presented in Figure 1.2(d). In this case, propane is much more soluble than methane, and so solubility selectivity favors propane [28]. However, propane is larger than methane, and so diffusion selectivity favors methane. In strongly size-sieving polymers (e.g. aromatic polyimides, aromatic polyamides, polysulfones, etc.), the diffusion selectivity is so high that it overwhelms the solubility selectivity,

and, therefore, these materials are methane-selective ($\alpha_{C_3H_8/CH_4} < 1$). However, many rubbery and certain ultrahigh-free-volume glassy polymers have very weak size-sieving ability, and so solubility selectivity dominates, and these materials are propane-selective ($\alpha_{C_3H_8/CH_4} > 1$). In any event, as materials become more permeable to propane, their propane/methane selectivity increases. In these cases, permeability and selectivity increase together, rather than opposing one another. Qualitatively, propane permeability is higher in materials (such as very flexible rubbery polymers (e.g. polydimethylsiloxane) or ultrahigh-free-volume polymers (e.g. poly(1-trimethylsilyl-1-propyne)) having a very high propane diffusion coefficient. Such materials tend to be weakly size-sieving, and so the diffusivity selectivity, which would always favor methane, the smaller molecule, would be weaker than the solubility selectivity in favor of propane [28]. Thus, as one systematically explores a series of materials of higher and higher propane permeability (due to higher and higher gas diffusion coefficients), one could generally expect to observe higher and higher propane/methane selectivity (as $D_{C_3H_8}/D_{CH_4}$ becomes closer to 1 in materials with higher diffusion coefficients and, in turn, weaker size-sieving ability).

1.2 Effects of Gas and Polymer Properties on Transport Coefficients

As indicated earlier, permeability is an intrinsic property of a gas–polymer system. Gases are much simpler materials than polymers, and so correlations are available to relate diffusion and solubility coefficients (and, hence, permeability values) of different gases in a given polymer. The situation with polymers is more complex. Nevertheless, some properties of polymers also correlate with the D, S and P values for a given gas, which has given rise to group contribution models aimed at predicting the permeability of polymers to gases [29–31]. However, universal correlations are typically worse than those valid for limited sets of polymers, such as, for example, rubbers and glasses, certain chemically similar classes of polymers, etc.; this limitation on such approaches reflects our lack of complete understanding of the detailed relation between polymer structure and gas transport properties. The sections below outline the most common approaches used to correlate gas and vapor sorption and transport properties in polymers.

1.2.1 Effect of Gas Properties on Solubility and Diffusivity

The diffusion coefficients of gas molecules characterize their dynamics or mobility in a polymer, and diffusion coefficients generally increase as gas molecule size decreases. As shown in Figure 1.3, for both rigid, glassy polymers and flexible, rubbery polymers, the square of a characteristic dimension of a penetrant molecule, d^2, is most often used as a scaling parameter for the logarithm of D [32–39]. This dependence arises from models such as the one developed by Meares, which supposes that the activation energy of diffusion is proportional to the effective cross-sectional area of the gas molecules [40]. More rarely, diffusion coefficients have been correlated with d or d^3 [41]. Linear correlations of the logarithm of D with d^2 are especially good for roughly spherical molecules, such as inert gases.

Different scales can be used for estimating the effective penetrant diameter, d, important for gas diffusion in polymers. There is no obvious single choice for effective molecular diameter that is both easily traceable to fundamental molecular properties and provides a scale for molecular size so that diffusion coefficients reliably decrease as molecular size increases. One might argue that such a universal scale cannot exist when, for example, polar or quadrupolar gases (e.g. CO_2, H_2S, H_2O, etc.) diffuse in polymer matrices that either promote aggregation of penetrants (e.g. H_2O in hydrophobic polymers) [42–44] or provide sites for strong and favorable interactions with the gases, such as CO_2 diffusion in amine-containing polymers [45]. However, in many cases, such strong interaction effects are not present, and diffusion coefficients of gases should decrease systematically with an appropriate and increasing measure of penetrant size.

The most widely used scales of penetrant size for gas diffusion are the so-called kinetic diameter, d_k, and the Lennard–Jones collision diameter, d_{LJ}, determined from gas viscosity or second virial coefficient data [22,46]. Widely quoted values of kinetic diameter are from the book by Breck, and these values are recorded for a number of gases in Table 1.1 [22,47]. Lennard–Jones collision diameter values are

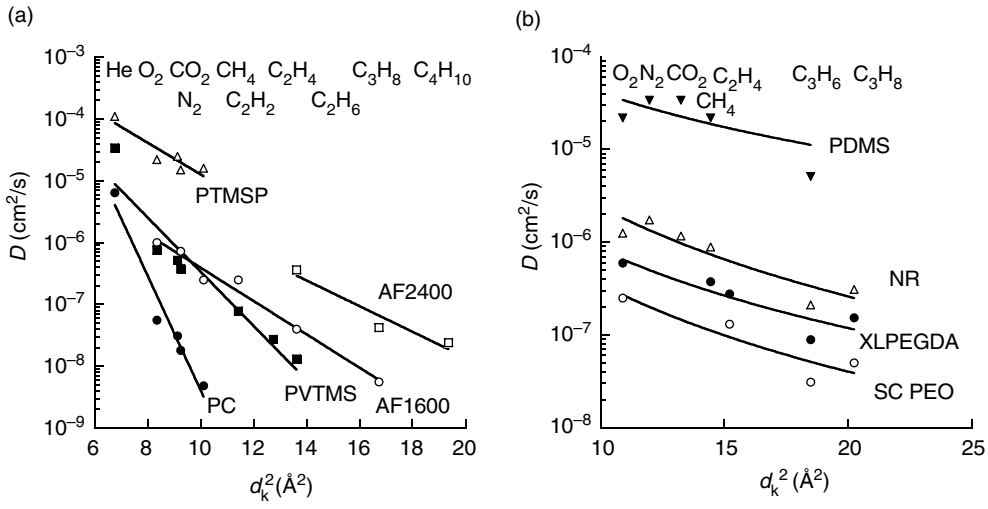


Figure 1.3 Dependence of diffusion coefficients on penetrant kinetic diameter in (a) glassy polymers at 23 °C, including poly(1-trimethylsilyl-1-propyne) (PTMSP), polyvinyltrimethylsilane (PVTMS), polycarbonate (PC), perfluorocarbon copolymers of 2,2-bis(trifluoromethyl)-4,5-difluoro-1,3-dioxole (BDD) and tetrafluoroethylene (TFE) containing 65 mol% BDD (AF1600) and 87 mol% BDD (AF2400) [39], and (b) rubbery polymers including cross-linked poly(ethylene glycol diacrylate) (XLPEGDA) at 35 °C [101], semicrystalline poly(ethylene oxide) (SC PEO) at 35 °C [32], natural rubber (NR) at 25 °C [33] and polydimethylsiloxane (PDMS) at 35 °C [34]. (a) Reprinted with permission from V. P. Shantarovich *et al*., *Macromolecules*, **33**, 7453–7466 (2000). Copyright (2000) American Chemical Society. (b) (i) Reprinted from *Journal of Membrane Science*, **239**, H. Lin and B. D. Freeman, 'Gas solubility, diffusivity and permeability in poly(ethylene oxide)', 105–117, Copyright (2004), with permission from Elsevier; (ii) From 'Flow of gases through polyethylene', A. S. Michaels and H. J. Bixler, *J. Polym. Sci*., **50**, 412–439, Copyright © 1961, John Wiley & Sons, Inc. Reprinted with permission of John Wiley & Sons, Inc.; (iii) From 'Gas sorption, diffusion and permeation in polydimethylsiloxane', T. C. Merkel, V. Bondar, K. Nagai, B. D. Freeman and I. Pinnau, *J. Polym. Sci. Part B: Polym. Phys. Ed.*, **38**, 415–434, Copyright © 2000, John Wiley & Sons, Inc. Reprinted with permission of John Wiley & Sons, Inc.; (iv) Reprinted with permission from H. Lin and B. D. Freeman, *Macromolecules*, **38**, 8394–8407 (2005). Copyright (2005) American Chemical Society

also used frequently in the literature, and so they are also reported in Table 1.1 for comparison [48]. As explained below, these two scales are quite closely related. An additional penetrant size scale is also reported in Table 1.1; this is based on a correlation due to Chung et al., which relates Lennard–Jones collision diameter to penetrant critical volume [48–50].

Because there appears to be some confusion in the literature regarding these penetrant size scales, a short discussion of their molecular basis is provided. The collision diameter is the intermolecular separation between two molecules of the same gas when the potential energy of interaction (calculated from the Lennard–Jones potential energy model) is equal to zero [51]. Many of the values referred to as kinetic diameter, d_k, in Breck [22] are, in fact, Lennard–Jones collision diameters reported in Hirschfelder, Curtiss and Bird (HCB) [51]. In fact, all of the values reported as kinetic diameters in Breck that are from HCB (Ar, O_2, N_2, Kr, Xe, CH_4, CF_4 and SF_6) are Lennard–Jones collision diameters that were originally determined using second virial coefficient data (i.e. *not* gas viscosity data). The kinetic diameters reported in Breck for H_2O and NH_3 (i.e. polar gases) are the collision diameters from the Stockmeyer potential model for polar substances, which is the distance of separation between two identical molecules at which the potential energy of interaction would be zero in the absence of dipole forces; these parameters were determined by fitting second virial coefficient data to the Stockmeyer potential [52]. The value reported as the kinetic diameter by Breck for CO_2, 3.3 Å, is significantly lower than the Lennard–Jones collision diameter considered by Breck (4.05 Å); Breck rationalizes the lower

value based on the observation that KA zeolite (KA zeolites contain AlO_4/SiO_4 at a 1 : 1 ratio and potassium cations) [22] adsorbs CO_2 but not N_2, which has a kinetic diameter of 3.64 Å. Breck argues that, for CO_2 to adsorb into this zeolite, it must have a kinetic diameter smaller than that of N_2. He also asserts that adsorption phenomena suggest that the critical molecular dimension characterizing whether or not a molecule will adsorb into a zeolite is the so-called minimum equilibrium separation, r_{min}, (i.e. the separation distance corresponding to the maximum attractive energy from the Lennard–Jones potential). He uses a value of 3.7 Å for the minimum equilibrium separation for CO_2 and the known relation between r_{min} and d_k ($r_{min} = 2^{1/6}d_k$) to calculate an effective kinetic diameter for CO_2 of 3.3 Å, which is a value widely quoted when CO_2 diffusion properties in polymers are discussed. This strategy was used in several cases by Breck to estimate effective kinetic diameters for gas molecules, including most of the hydrocarbons considered by Breck.

Several shortcomings of the above procedure are evident. First, when the effective gas molecular size is estimated from Lennard–Jones parameters, there is no systematic accounting for the influence of molecular shape anisotropy on effective molecular size since such effects are not included in the Lennard–Jones model. This issue may have stimulated Breck to propose the alternative procedure described above for CO_2. Secondly, the Lennard–Jones parameters determined from gas viscosity (i.e. transport) data and from second virial coefficient (i.e. thermodynamic) data for the same gas often show significant differences [53]. In a related issue, often several sets of fairly different Lennard–Jones parameters can be found that offer an essentially equivalent fit to the underlying experimental data [48]. Both of these effects frustrate the identification of a unique effective molecular diameter based on such data.

These shortcomings have led to a number of alternative proposals of effective molecular size appropriate for correlating diffusion coefficients [54,55]. For example, a special scale convenient for prediction of gas diffusivity in polymers was suggested [37,38]. However, the gas diameters from this scale do not give good predictions of upper bound relations when they are used in models to predict such phenomena [21]. For a homologous series of penetrants (e.g. *n*-alkanes), it is convenient and simple to use a single parameter, such as the number of carbon atoms in the molecule, because this provides a convenient (albeit empirical) and simple way to prepare correlations for *D* and, in many cases, *P*, with gas size [56–58], as shown in Figure 1.4. For the light gases (i.e. H_2, He, N_2, O_2, CH_4 and CO_2), kinetic diameter gives the most faithful scaling of diffusion coefficients with penetrant size [22]. However, for larger gas molecules, kinetic diameter breaks down as a useful scaling parameter for penetrant size. For example, as shown in Table 1.1, the kinetic diameters of propane and *n*-butane are equal (4.3 Å). This result is consistent with the methodology used by Breck to estimate these kinetic diameters; as indicated above, the calculation was based on the minimum molecular width, which is the same for propane and *n*-butane [22]. However, diffusion coefficients of *n*-butane are always lower than those of propane in any polymer, which indicates that both molecular length and width influence diffusion coefficients;

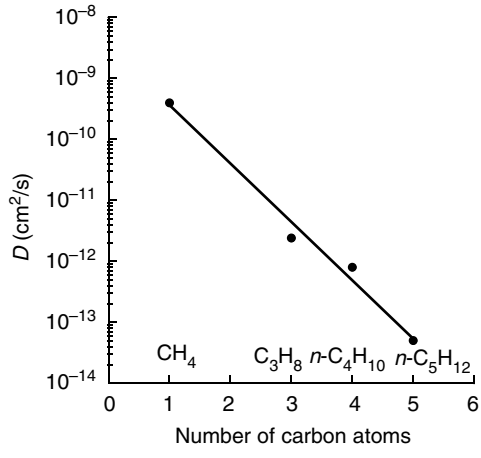


Figure 1.4 Infinite-dilution, estimated amorphous-phase diffusion coefficients of linear alkane hydrocarbons in poly(ethylene terephthalate) at 25 °C [14,58]. (i) Reprinted with permission from S. N. Dhoot *et al.*, *Industrial and Engineering Research*, **43**, 2966–2976 (2004). Copyright (2004) American Chemical Society; (ii) From 'Sorption and transport of linear alkane hydrocarbons in biaxially oriented poly(ethylene terephthalate)', S. N. Dhoot, B. D. Freeman, M. Stewart and A. J. Hill, *J. Polym. Sci. Part B: Polym. Phys. Ed.*, **43**, 1160–1172, Copyright © 2005, John Wiley & Sons, Inc. Reprinted with permission of John Wiley & Sons, Inc.

the longer *n*-butane diffuses slower than the shorter propane. As another example, the kinetic diameter of propylene (4.5 Å) is larger than that of propane (4.3 Å), even though propylene diffusion coefficients are always higher than those of propane [59]. Additionally, only a limited set of kinetic diameter (d_k) values have been proposed [22], and so kinetic diameter values are not available for all penetrants of interest.

If many penetrants of varying size and shape are considered, estimates of size such as the van der Waals volume or critical volume are often more convenient scaling parameters since these values are available for practically any gas or vapor of interest [48]. The resulting empirical correlations often roughly obey a relation of the following form [60]:

$$D = \frac{\tau}{V_C^{\eta}} \tag{1.24}$$

where τ and η are polymer-dependent parameters, and V_C is the penetrant critical volume. Correlations such as this are only valid in the limit of low penetrant concentrations, when D is independent of penetrant concentration. Additionally, parameters such as critical volume do not carry any special shape-dependent information useful for correlating diffusion coefficients, and therefore such parameters should be used with care. Extrapolation beyond the range of penetrants studied, particularly to those of molecular shape markedly different from those used to establish the parameters of the correlation (e.g. branched versus unbranched penetrants), is not recommended and can lead to significant variance from the correlation [14]. Molecular diameters based on the Chung *et al*. model correlating collision diameter with critical volume are also provided in Table 1.1 in case a linear penetrant dimension is preferred over a volumetric measurement; since d_C and V_C are directly related. As indicated in the footnote of Table 1.1, there is no obvious advantage to using one or the other.

For many polymers, gas solubility coefficients over short ranges of penetrant critical temperature are well described by a linear relationship between the logarithm of S and some convenient measure of solute condensability, such as critical temperature, T_c, normal boiling point, T_b [61] or Lennard–Jones energy parameter, ε/k [31]. Two of these parameters, T_c and ε/k, are presented in Table 1.1 for common gases and vapors. An example of such a correlation is presented in Figure 1.5(a) for a rubbery polymer, polydimethylsiloxane (PDMS), and for a glassy polymer, poly(1-trimethylsilyl-1-propyne) (PTMSP). In the rubbery polymer, solubility of the light

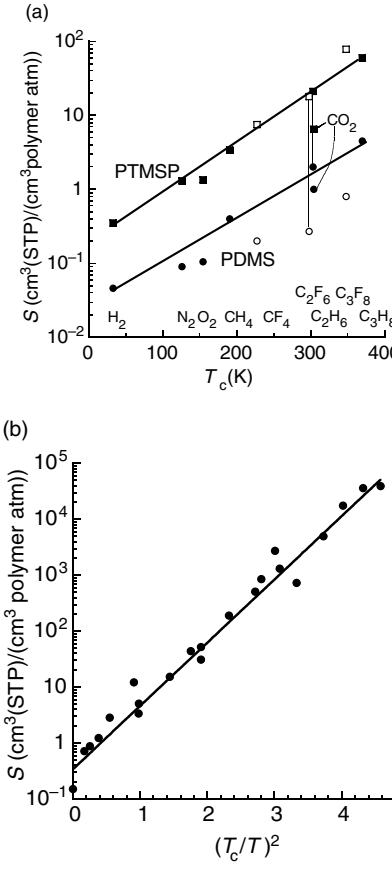


Figure 1.5 Correlation of low-pressure-limit solubility coefficients with solute critical temperature in (a) PTMSP and PDMS, and (b) AF2400 [12,88]. (a) From 'Sorption and transport of hydrocarbon and perfluorocarbon gases in poly(1-trimethylsilyl-1-propyne)', T. C. Merkel, V. Bondar, K. Nagai and B. D. Freeman, *J. Polym. Sci. Part B: Polym. Phys. Ed.*, **37**, 273–296, Copyright © 1999, John Wiley & Sons, Inc. Reprinted with permission of John Wiley & Sons, Inc. (b) (i) Reprinted with permission from V. Bondar *et al*., *Macromolecules*, **32**, 6163–6171 (1999). Copyright (1999) American Chemical Society; (ii) Reprinted with permission from T. C. Merkel *et al*., *Macromolecules*, **32**, 8427–8440 (1999). Copyright (1999) American Chemical Society

gases and hydrocarbons (closed symbols) follows solubility is singular a rather linear progression with increasing critical temperature. The fluorocarbon gases (open symbols) fall considerably below this line due to the unfavorable interactions between fluorocarbon gases and hydrocarbon-based polymers such as PDMS; this effect is discussed in more detail in the chapter by Merkel *et al.* in this book. This result demonstrates the applicability of such correlations and an example of their failure, when specific interactions between the polymer and penetrant become significant. In the high-free-volume glassy polymer, PTMSP, the unfavorable interactions between this hydrocarbon-based polymer and perfluorinated penetrants are less obvious than in the lower-free-volume rubber, PDMS; this lack of sensitivity to mismatches in polymer/penetrant interaction energies has been ascribed to the strong driving force, in the glassy polymer, to fill the unoccupied non-equilibrium excess free volume of the polymer with penetrant molecules [62]. At conditions far from infinite dilution, when the so-called Langmuir excess free volume sites of the glassy polymer are predominantly filled, PTMSP exhibits higher solubility for hydrocarbon penetrants than for fluorocarbons, more consistent with the behavior shown by PDMS [62].

The fundamental basis for gas solubility to scale with penetrant condensability follows from simple, classical solution thermodynamics [8,63]. The enthalpy of sorption, ΔH_s, in the van't Hoff equation for gas dissolution is [8]:

$$S = S_0 e^{-\Delta H_s/RT} \tag{1.25}$$

Historically, for both gas solubility in liquids [48] and polymers [8], the enthalpy of sorption can be thought of in terms of two contributions:

$$\Delta H_s = \Delta H_c + \Delta H_m \tag{1.26}$$

where ΔH_c is the enthalpy of condensation of the pure gaseous penetrant to the liquid phase or, for penetrants which are above their critical temperature at the measurement conditions, to a condensed density consistent with that of the polymer, and ΔH_m is the partial molar enthalpy of mixing the condensed (or compressed) penetrant with the polymer segments. The enthalpy of condensation of the penetrant is related to its enthalpy of vaporization: $\Delta H_V = -\Delta H_C$.

Table 1.2 Slope, a_c, of the linear relationship between 1n S and T_c for gas solubility in organic liquids at 20 °C [66]. Reprinted with permission from R. Prabbakar *et al.*, *Macromolecules*, **38,** 1899–1910 (2005). Copyright (2005) American Chemical Society

Solvent	$a_c \times 10^3 (K^{-1})$
Methyl alcohol	14
Ethyl alcohol	15
Amyl alcohol	16
Ethyl ether	14
Acetone	17
Methyl acetate	16
Ethyl acetate	15
Benzene	18
Toluene	14
Xylene	13
Cyclohexane	16
Cyclohexanol	13
Tetrachloromethane	15
Chloroform	19
Chlorobenzene	19

Experimentally, there are strong correlations between ΔH_V and any of several convenient scales of gas condensability [64]:

$$\Delta H_v/R = a_b T_b = a_c T_c = a_e(\varepsilon/k) \tag{1.27}$$

where a_b, a_c and a_e are all adjustable constants. If $|\Delta H_m| \ll |\Delta H_c|$, which is often the case for many gases [64,65], then:

$$\begin{aligned} \ln S &= \ln S_0 + a_b T_b = \ln S_0 + a_c T_c \\ &= \ln S_0 + a_e(\varepsilon/k) \end{aligned} \tag{1.28}$$

For most polymers and penetrants the values of a_c are quite similar. That is, a_c is a near-universal parameter. Similar behavior is observed for gas dissolution in liquids. To illustrate this point, Table 1.2 presents a_c values for many gases in a number of organic liquids; the solubility data used to determine these values of a_c range over three orders of magnitude, depending on the gas [66,67].

Gas solubility in polymers obeys similar trends to those observed in liquids. That is, a_c is approximately independent of polymer chemical structure, as shown in Table 1.3 [67–72]. In fact, a comparison of the values in Tables 1.2 and 1.3 indicate that the values of a_c are very similar for gases dissolving in liquids and in

Table 1.3 Slope, a_c, of the linear relationship between ln S and T_c for gas solubility in polymers. Reprinted from *Polymer*, **42**, G. E. Serad, B. D. Freeman, M. E. Stewart and A. J. Hill, 'Gas and vapor sorption and diffusion in poly(ethylene terephthalate)', 6929–6943, Copyright (2001), with permission from Elsevier

Classification	Medium	$a_c \times 10^3 (K^{-1})$
Rubbers	Natural rubber [70]	18[a]
	Amorphous polyethylene [70]	16[a]
	Polybutadiene – hydrogenated [70]	17[a]
	Polydimethylsiloxane [68]	17[b]
Glassy polymers	Polysulfone [72]	17[c]
	Poly(phenylene oxide) [69]	16[d]
	Poly(ethylene terephthalate) [71]	19[e]

[a] 25 °C and 1 atm.
[b] 35 °C
[c] 35 °C and 10 atm for all gases, except n-C_4H_{10}, which is at infinite dilution.
[d] 35 °C and infinite dilution.
[e] 24–45 °C and infinite dilution.

polymers, which underscores the similarity of gas dissolution in liquids and polymers. Exceptions to the general rule that a_c is independent of polymer structure occur in fluorocarbon/hydrocarbon mixtures [67]. Complications may arise for glassy polymers and for solutes (in both rubbery and glassy polymers) with large values of ΔH_m. In glassy polymers, partial molar enthalpies of sorption are often negative and can differ significantly from zero [12]. Moreover, ΔH_m values in glassy polymers are typically concentration-dependent, particularly for strongly sorbing components. In both glassy and rubbery polymers, for more condensable (i.e. heavier) solutes, such as higher hydrocarbons and organic vapors, $|\Delta H_c| > |\Delta H_m|$, and ΔH_c is directly proportional to T_c^2 [73]. For such cases, correlations of the following type have been proposed [12,74]:

$$\ln S = M + NT_c^2 \tag{1.29}$$

$$\ln S = M' + N'(T_c/T)^2 \tag{1.30}$$

An example of such a correlation is shown in Figure 1.5(b). However, for studies involving only light gases, the correlations given by Equation (1.28) (i.e. solubility scaling with T_c) are obeyed with sufficient accuracy to be used for correlating solubility.

If van der Waals forces dominate gas–polymer interactions during dissolution, then solubility coefficients have also been linked to appropriately defined surface areas of molecules. Good correlations between ln S, van der Waals surface areas, as estimated using (UNIFAC), and solvent accessible surface areas have been demonstrated for numerous polymers (both rubbery and glassy) [75]. In contrast to Equation (1.8), these correlations are linear for a wide range of solutes.

In a series of penetrants, as the size of the diffusing molecules increases, the D values decrease. On the other hand, for many penetrants, T_c increases (roughly) as penetrant size increases, and so S often increases as the penetrant size increases. The resulting permeability coefficients reflect these often competing trends in D and S with increasing penetrant size. Water is a notable exception to these trends. It has a very high T_c value (647.3 K [48]) and a small kinetic diameter value, 2.65 Å [22], making it often the most permeable gas in a polymer.

As illustrated in Figure 1.3, the slopes of the dependence of D on d^2, or the size-sieving ability of the polymer, can be quite different for polymers in the rubbery and glassy states. All other factors being equal, for polymers above their glass transition temperatures (T_g), D is often less sensitive to penetrant size than in traditional, stiff-chain, low-free-volume glassy polymers because polymers with higher molecular chain mobility (i.e. lower T_g) tend to provide larger and more frequent availability of free volume elements of sufficient size to accommodate diffusion steps of both large and small penetrant molecules, which is the basis of their weaker size-sieving ability (i.e. D depends weakly on penetrant size). Low-free-volume, rigid, glassy polymers have very restricted chain motion, which provides small free-volume elements, suitable for diffusion steps of small gases, much more often than free-volume elements large enough to allow diffusion of larger gas molecules; the large disparity in the availability of free-volume elements suitable for small and large penetrants leads to strong size-sieving ability (i.e. a strong dependence of D on penetrant size). However, in addition to the influence of molecular mobility on diffusion coefficients and size-selectivity, there is a substantial

influence of free volume on both D and diffusivity selectivity. As discussed in Chapter 11, diffusivity selectivity increases as the size of free-volume elements in the polymer decreases. These two effects (chain mobility, as characterized by T_g, and free volume) can oppose one another so that, for example, materials with higher T_g values, high diffusion coefficients and stronger size-sieving ability can be prepared [76].

If one uses a single scaling parameter for correlations involving D, S and P (e.g. V_c, the gas critical volume) (cf. Figure 1.6), then for

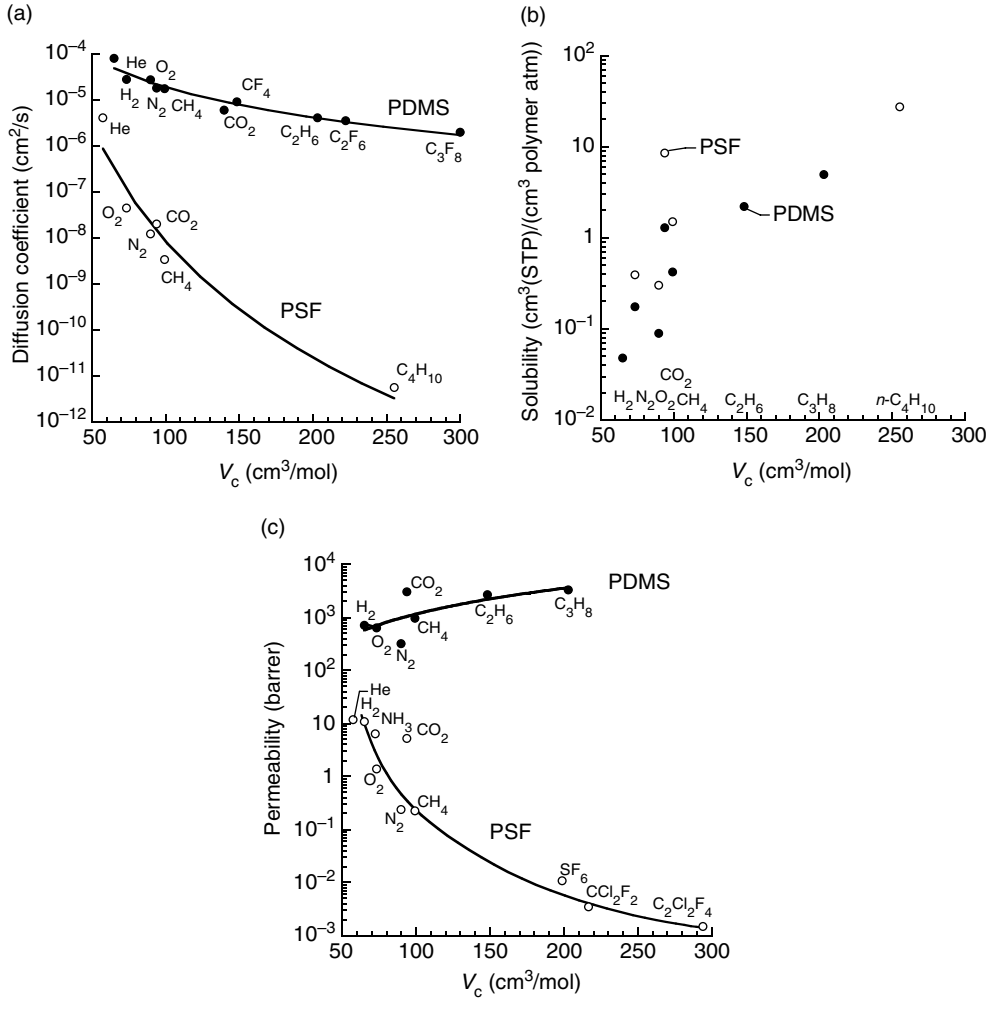


Figure 1.6 Correlations of (a) diffusion, (b) solubility and (c) permeability values with penetrant critical volume in polysulfone (PSF) and PDMS [34,45]. Solubility and permeability experiments were conducted at an upstream pressure between 3 and 20 atm for all penetrants, except for *n*-butane which was conducted at an upstream pressure of less than 1 atm. The downstream pressure was 'at vacuum' and atmospheric pressure for PSF and PDMS, respectively. Diffusion coefficients were calculated from the permeability and solubility data, while PSF and PDMS data were collected at 23 and 35 °C, respectively. (a–c) (i) From 'Gas sorption, diffusion and permeation in polydimethylsiloxane', T. C. Merkel, V. Bondar, K. Nagai, B. D. Freeman and I. Pinnau, *J. Polym. Sci. Part B: Polym. Phys. Ed.*, **38**, 415–434, Copyright © 2000, John Wiley & Sons, Inc. Reprinted with permission of John Wiley & Sons, Inc.; (ii) Reprinted with permission from K. Ghosal *et al*., *Macromolecules*, **29**, 4360–4369 (1996). Copyright (1996) American Chemical Society

low-free-volume conventional glassy polymers, such as polysulfone, similar dependences of D and P on V_c are observed. As illustrated by this example, solubility is not correlated nearly as well with V_c as with T_c. Therefore, in membranes based on conventional, low-free-volume glassy polymeric materials (e.g. polysulfone), the smaller, faster diffusing components of the feed mixture is always enriched in the permeate. In contrast, in some flexible, high-free-volume rubbers, such as PDMS, the dependence of P on V_c is similar to the effect of S on V_c (cf. Figure 1.6). In such a membrane, permeate streams are enriched in the heavier (i.e. larger, more soluble) components in the feed stream. Although not all rubbery polymers exhibit such 'reverse-selective' properties, PDMS has high permeability and organic–vapor/gas selectivity, and is used commercially as a membrane for separations requiring this capability [28].

A notable exception from the regularity described above is PTMSP and the related highly permeable, substituted acetylene polymers discussed in detail in Chapter 9. These rigid, glassy polymers are characterized by very high levels of free volume, which contribute to extremely high diffusion coefficients and very weak size-sieving ability. Hence, in these polymers, larger, more soluble penetrants are more permeable than smaller, less soluble penetrants. Membranes based on such materials could be used for enrichment of the heavier components of gas streams, (e.g. removal of higher hydrocarbons from natural gas), if other requirements are fulfilled, such as long-term stability of permeability and chemical stability in the feed streams to be separated [77,78].

1.2.2 Effect of Polymer Properties on Transport Parameters

1.2.2.1 Glass Transition Temperature

The effects of the T_g on permeability and diffusivity are especially evident for rubbers or semicrystalline polyolefins when the T_g is below room temperature. In elastomers, polymer segmental mobility creates the transient free-volume elements that allow gas and vapor diffusion through the polymer to occur. Free volume in such media, like in liquids, undergoes rapid fluctuations, and so the difference between the measurement temperature, T_m, and T_g has a strong effect on free volume and serves as a crude indicator of segmental mobility at T_m. Indeed, good correlations of D and P with T_g have been demonstrated by several authors [36,79,80], while the S values are essentially independent of T_g. Example of such correlations for D and P are shown in Figure 1.7.

While there is a general trend evident in these figures, there is also quite a bit of scatter, suggesting that factors other than T_g contribute in an important way to diffusivity and permeability. Side-chain mobility can also affect the T_g values and, in turn, the transport parameters [81,82]. In glassy polymers, increasing T_g in a group of structurally related glassy polymers (e.g. by adding substituents to the aromatic rings of low-free-volume, aromatic polysulfones) often results in increases in P and D [76]. As such, attempts to find general correlation between glass transition temperature in glassy polymers and permeation properties failed (e.g. see Hirayama *et al.* [83]). For example, high-T_g polymers can display very large (e.g. PTMSP [84]) and rather small (e.g. Kapton polyimide [85]) diffusivity and permeability values. However, this phenomenon can be explained by the complex nature of factors that influence gas diffusion and permeability. Diffusion coefficients are exquisitely sensitive to free volume in a polymer. However, free volume is only one of several factors that affect T_g, which depends on both intermolecular interactions (which may be sensitive to free volume) and intramolecular interactions (which may depend more on the energy barriers to rotation about backbone covalent bonds than on free volume). Hence, correlations of gas diffusivity or permeability with T_g often do not characterize the free volume or its distribution adequately as they relate to diffusion properties. Consequently, free volume is usually viewed as more relevant than T_g for correlating transport properties in polymers.

In addition to the rather large-scale segmental mobility that is important in T_g-type motions of polymer chains, smaller-scale main- or side-chain motions that determine sub-T_g behavior also influence gas permeation in polymers. In fact, low-temperature transitions (e.g. T_γ) in substituted polysulfones correlate well with gas permeability coefficients. However, this correlation derives from intramolecular packing or free-volume effects that change both T_γ and P in

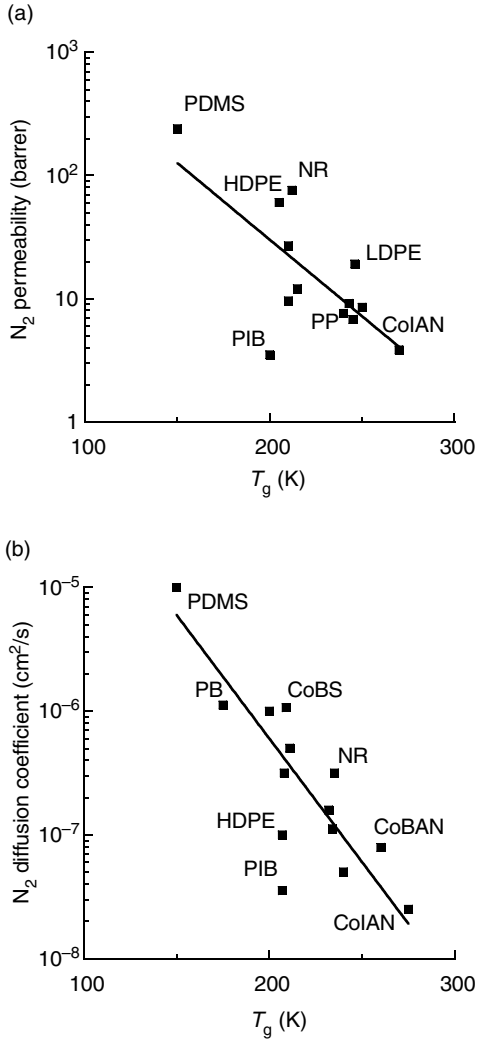


Figure 1.7 (a) Permeability and (b) diffusion coefficients for nitrogen in rubbers with different glass transition temperatures: polydimethylsiloxane (PDMS), high-density polyethylene (HDPE), low-density polyethylene (LDPE), natural rubber (NR), polyisobutylene (PIB), polypropylene (PP), polybutadiene (PB), poly(butadiene-*co*-styrene) (CoBS), poly(isoprene-*co*-acrylonitrile) (CoIAN), poly(butadiene-*co*-acrylonitrile) (CoBAN), methyl rubber (MR) and polychloroprene (PCP). Experiments were conducted at room temperature and in a pressure range where P and D are independent of pressure [79]. (a, b) Reproduced by permission of 'Nauka' RAN, Moscow from Y. P. Yampolskii, S. G. Durgaryan and N. S. Nametkin, 'Translational and rotational mobility of low molecular mass compounds in polymers with different glass transition temperatures', *Vysokomolekuliarnye Soedineniia*, **24**, 536–541 (1982)

similar ways [76], suggesting a subtle interplay between local polymer chain mobility, chain packing and gas transport properties.

1.2.2.2 Molecular Mass

The molecular mass of polymers typically does not significantly influence the gas permeation parameters. That is, chain end-groups rarely exert a significant influence on the transport properties. At low molecular weights, where one might anticipate the strongest effects of molecular weight, it is often difficult to prepare mechanically stable, free-standing films; at molecular weights high enough to prepare films which can undergo permeation testing, the effect of molecular weight on the transport properties is usually small. In this regard, the literature reports fairly weak effects of polymer molecular mass on P and D values (e.g. see [86–88]). Toi and Paul reported some variation in the solubility coefficient of CO_2 in polystyrene samples with molecular masses in the range of 3600 to 850 000 [89]. However, these effects can be partly ascribed to a concomitant increase in T_g from 345 to 374 K. The situation is different in cross-linked rubbery polymers; in these materials, chain end-groups can be introduced via pendant side-chains, while mechanical properties can be controlled somewhat independently by varying the cross-linking density. Thus, it is possible to prepare mechanically robust materials with high concentrations of chain-ends. Lin *et al.* have observed strong effects of chain-end concentration on transport properties in such systems [90], where increasing chain end $-OCH_3$ concentration in poly(ethylene glycol) network polymers from essentially 0 wt% of total sample mass to 6.7 wt% increases the CO_2 diffusivity fivefold [90].

Permeability is sensitive to various parameters that characterize chain packing, such as polymer density [91] or mean interchain distance (d-spacing deduced from wide-angle X-ray diffraction (WAXD) studies) [83,92]. However, the most relevant measure of chain packing efficiency is *free volume*. According to free-volume theory [5]:

$$D = A_0 \exp\left(-\frac{\gamma V^*}{V_f}\right) \tag{1.31}$$

where A is a prefactor, V_f is the average free volume in the system, γ is a parameter of order unity introduced to prevent double counting of free-volume elements in the theory leading to this equation, and V^* characterizes the size of diffusing molecules; to be coherent with the correlations described earlier and with emerging experimental data related to this issue, γV^* is often found to be proportional to d^2.

Chapters 3, 4 and 7 in this volume discuss at length many of the definitions and methods for determining free volume in polymers. The simplest and most popular way employs the definition suggested by Bondi [93]. According to this method, the specific free volume in a polymer, V_f (cm^3/g), is the difference between the specific volume of a polymer, $V_{sp} = 1/\rho$, where ρ (g/cm^3) is the polymer density, and its occupied volume, V_{oc}. Bondi proposed calculating V_{oc} as $1.3\,V_w$, where V_w is the sum of the increments of van der Waals volumes (values tabulated in van Krevelen [31]). Hence:

$$V_f = V_{sp} - 1.3\,V_w \tag{1.32}$$

In most cases, a dimensionless, reduced value of the free volume, called the fractional free volume ($FFV = V_f/V_{sp}$), gives better correlations than V_f with transport properties within a family of polymers. Thus, it is most common to replace V_f in Equation (1.31) with FFV:

$$D = A e^{-B/FFV} \tag{1.33}$$

where A and B are empirical constants which vary from gas to gas and from one polymer to another. Based on the arguments given above for γV^*, B should be expected to scale with some measure of penetrant size. Strictly speaking, this equation applies only to the gas self-diffusion coefficient [94,95]. However, from a practical viewpoint, since the concentration of gas in the polymer is typically less than 10 vol%, the correction factor between the self-diffusion coefficient and the mutual-diffusion coefficient is typically small. As a result, in the gas transport field, the key result from free volume theory (Equation (1.33)) is usually applied directly to mutual-diffusion coefficients, and we adopt that approach here.

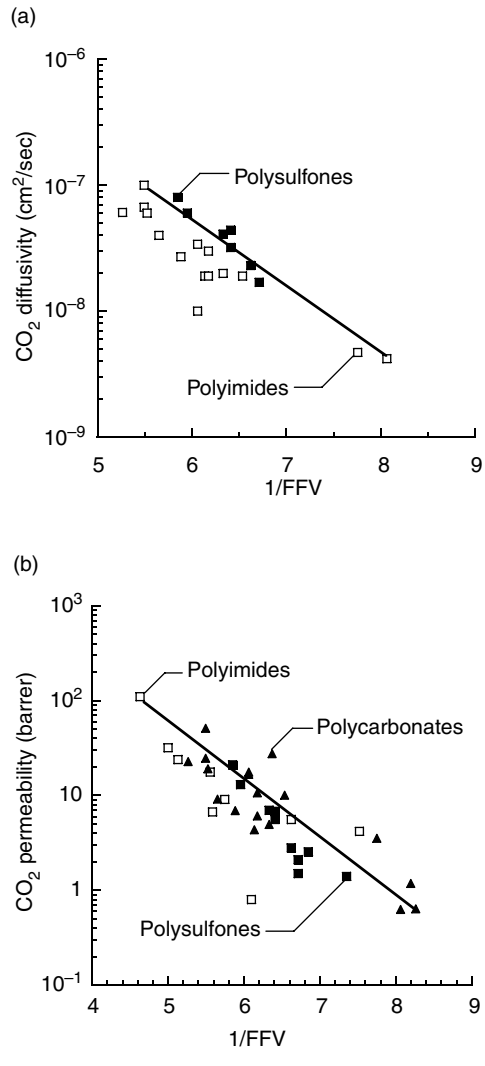


Figure 1.8 Correlations of (a) CO_2 diffusion and (b) CO_2 permeability coefficients with fractional free volume in glassy aromatic polysulfones, polyimides and polycarbonates. The experiments were conducted at 35 °C, a feed pressure of 10 atm while the permeate pressure was 'at vacuum' [76]

Figure 1.8 presents an example of such a correlation of mutual diffusion coefficients with fractional free volume. Gas solubility coefficients in polymers vary over a much narrower range than diffusivity, and the effect of free volume on solubility is generally much weaker than on diffusivity. Therefore, gas permeability coefficients are

often directly correlated with fractional free volume [54]:

$$P = A_P e^{-B/FFV} \tag{1.34}$$

where, to be consistent with Equation (1.9), $A_P = SA$. A correlation of this type is presented for CO_2 in Figure 1.8(b).

For reasons discussed in Chapter 7, the Bondi method gives rather rough estimates of the influence of free volume upon gas diffusion and permeation properties in polymers. Good correlations for P and D are usually obtained for structurally related polymers (e.g. Figures 1.8(a) and 1.8(b)), whereas attempts to draw predictable correlations for extensive sets of polymers from very different families of polymers show more scatter (cf. Figure 1.9) [96–100]. It has been suggested that systematic errors in the van der Waals increments might lead to such discrepancies among widely varying families of polymers. One method for checking the validity of Equations (1.28) and (1.29) might be to examine the dependence of P and D on FFV for gases with different molecular dimensions. In rubbery polymers, recent results by Lin and Freeman have shown remarkably strong correlations between B and penetrant size for a series of rubbery polymers. An example of such a correlation is presented in Figure 1.10 [101].

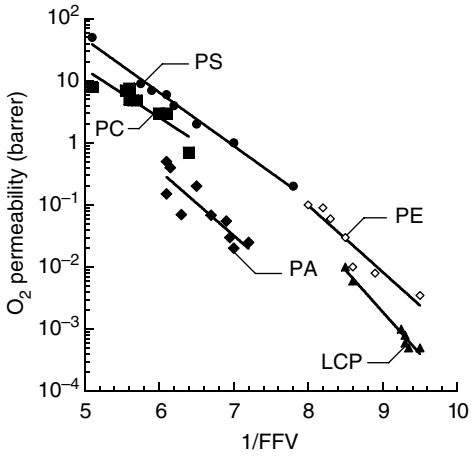


Figure 1.9 O_2 permeability for glassy polystyrenes (PS) at 35 °C [96], polycarbonates (PC) at 35 °C [97,170], polyamides (PA) at 25 °C [54], polyesters (PE) at 30 °C [98] and liquid crystalline polyesters (LCP) at 35 °C [99,100]

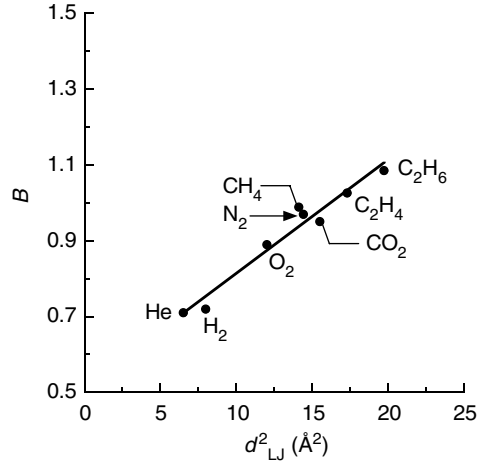


Figure 1.10 The dependence of B on penetrant Lennard–Jones diameter squared in cross-linked poly(ethylene glycol diacrylate), the equation for the best-fit line is $B = 0.51 + 0.030\,d_{LJ}^2$ when the units of d_{LJ} are Å [101]. Reprinted with permission from H. Lin and B. D. Freeman, *Macromolecules*, **38**, 8394–8407 (2005). Copyright (2005) American Chemical Society

However, in glassy polymers, only approximate correlations between diffusivity and permeability with free volume have been observed when Bondi's method is used to estimate FFV [102,103]. Better correlations can be obtained after accounting for interchain interactions (cohesive energy density) or via direct determination of free volume in polymers using, for example, positron annihilation lifetime spectroscopy [103,104]. Gas diffusion in polymers should be hampered by strong interchain interactions, and so cohesive energy density (CED = E_{coh}/V_{sp}) [31] can be included in correlations such as those described earlier to improve the correlation [103]. A simple equation:

$$\log P = A' - B'(CED/FFV) \tag{1.35}$$

has been proposed to account for interchain interactions in gas-transport-impacting glassy polymers [105].

1.3 Effect of Pressure on Transport Parameters

1.3.1 Sorption

Figure 1.11 shows schematically the basic isotherm shapes that are often observed. The simplest behavior is presented in Figure 1.11(a), which shows the sorption isotherm of O_2 in rubbery polydimethylsiloxane (PDMS). These linear isotherms obey Henry's law, and are characterized in terms of a Henry's law parameter, k_D, which is defined as follows:

$$C = k_D p \tag{1.36}$$

Such isotherms are observed for light gas (e.g. He, H_2, N_2, O_2, CH_4) sorption in rubbery polymers at essentially all pressures of practical interest.

For more condensable gases (e.g. CO_2, higher hydrocarbons and vapors), at sufficiently high pressure (typically pressures that are significant relative to the vapor pressure for penetrants below their critical temperature), strong deviation from Henry's law and, consequently, non-linear sorption isotherms are observed. A sorption isotherm which is convex to the pressure axis is characteristic of vapor dissolution in polymers above their glass transition temperatures and is historically described by using the Flory–Huggins equation [8]:

$$\ln a = \ln (p/p_s) = \ln \phi_v + (1 - \phi_v) + \chi(1 - \phi_v)^2 \tag{1.37}$$

where a is penetrant activity in the gas phase contiguous to the polymers, p and p_s are the pressure and saturation vapor pressures of the gas, respectively, ϕ_v is the volume fraction of penetrant dissolved in the polymer, and χ is the so-called Flory–Huggins interaction parameter. The first equality in Equation (1.37) ($a = p/p_s$) presumes that the gas phase is ideal, which can be relaxed by using an appropriate equation of state if the gas phase is non-ideal. When $\chi > 2$, polymer–gas interactions are small, and if $\chi \leq 0.5$ interactions are so strong that non-cross-linked polymer can dissolve in the penetrant. Figure 1.11(b) provides an example (acetone sorption in PDMS) where the Flory–Huggins model has been used to describe the experimental data [106]. Although the polymer presented in Figure 1.11(b) (PDMS) is cross-linked, the cross-linking has not been accounted for in the sorption data analysis. For cases of typical interest in gas and vapor separations, cross-linked polymers such as PDMS often do not sorb sufficient amounts of penetrants for the elastic constraints imposed by the cross-linked network to have a significant influence on the penetrant chemical potential. That is, the terms in, for example, the Flory–Rehner model [107,108] which would account for the effect of cross-linking on the gas sorption level in a polymer, are typically negligible. Another typical case where isotherms are convex to the pressure or activity axis is realized in sorption of water or lower alcohols into hydrophobic polymers [42,43,109,110]. These isotherms are evidence of solute cluster formation, which becomes progressively more important at higher activity. One drawback of the Flory–Huggins model is that, to successfully describe the experimental data, χ often must be treated as an empirical parameter that depends on temperature and penetrant concentration. Recently, more effort has focused on using more modern equations of state, such as the Sanchez–LaCombe equation, to model sorption in rubbery polymers in an attempt to improve the ability to model sorption properties without relying on *ad hoc* empirical additions to the Flory–Huggins model [111].

Sorption isotherms which are concave to the pressure axis are typical for glassy polymers. An example is presented in Figure 1.11(c). The three-parameter dual-mode sorption isotherm model has been widely used to describe gas sorption in this case [112]:

$$C = k_D p + C'_H \frac{bp}{1 + bp} \tag{1.38}$$

where k_D is the Henry's law parameter characterizing sorption into the densified equilibrium matrix of the glassy polymer, C'_H is the Langmuir sorption capacity, which characterizes sorption into the non-equilibrium excess volume associated with the glassy state, and b is the Langmuir affinity parameter. In this model, two ''popula-

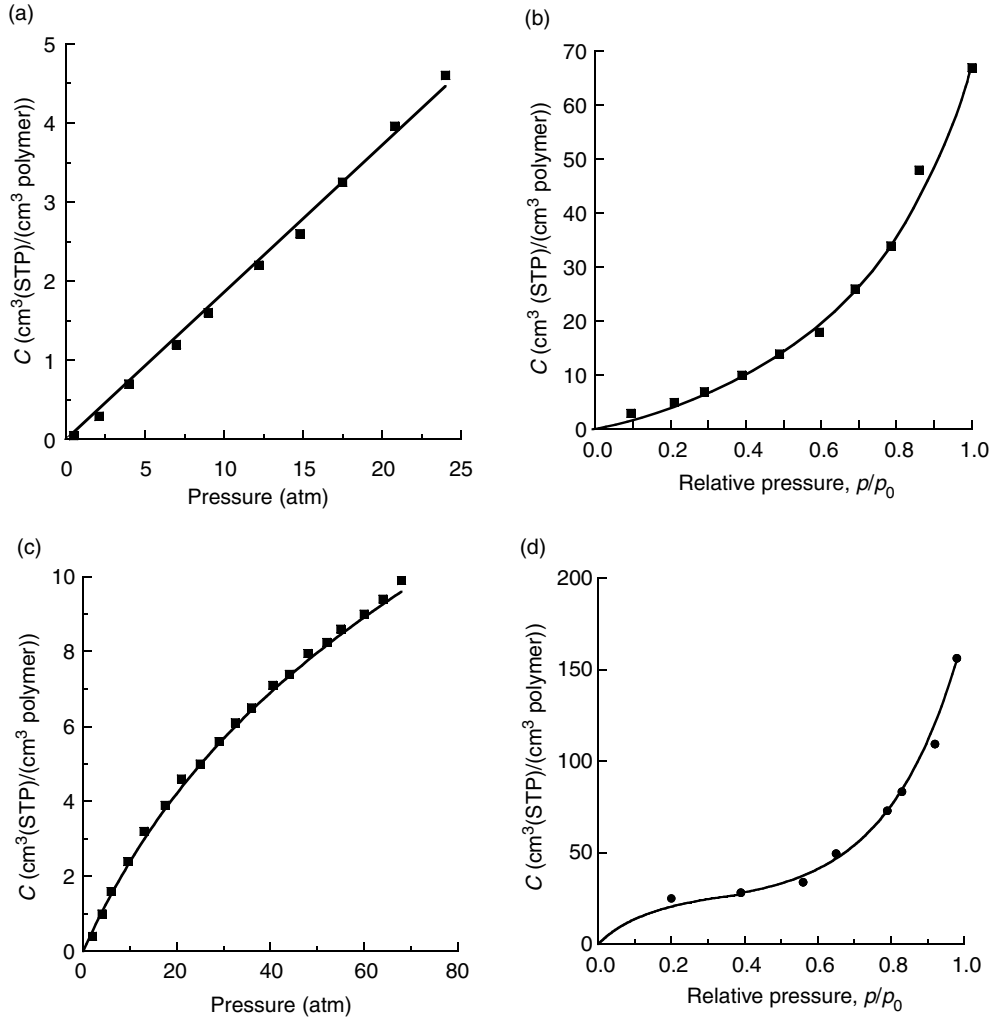


Figure 1.11 Typical gas sorption isotherms: (a) Henry's law (O_2 in PDMS at 35 °C [34]); (b) Flory–Huggins (FH) (acetone in PDMS at 28 °C [106]), where p_0 is the acetone vapor pressure, which is 258 mmHg at 28 °C; (c) dual-mode sorption (DMS) (Argon in PSF at 25 °C [120]); (d) DMS + FH (vinyl chloride monomer (VCM) in poly(vinyl chloride) (PVC)) at 30 °C [121] (p_0 is the VCM vapor pressure, which is 2980 mmHg at 30 °C). (a) From 'Gas sorption, diffusion and permeation in polydimethylsiloxane', T. C. Merkel, V. Bondar, K. Nagai, B. D. Freeman and I. Pinnau, *J. Polym. Sci. Part B: Polym. Phys. Ed.*, **38**, 415–434, Copyright © 2000, John Wiley & Sons, Inc. Reprinted with permission of John Wiley & Sons, Inc. (b) From 'Pure and mixed gas acetone/nitrogen permeation properties of polydimethylsiloxane', A. Singh, B. D. Freeman and I. Pinnau, *J. Polym. Sci. Part B: Polym. Phys. Ed.*, **36**, 289–301, Copyright © 1998, John Wiley & Sons, Inc. Reprinted with permission of John Wiley & Sons, Inc. (c) From 'On pressure dependence of the parameters of the dual-mode sorption model', V. Bondar, Y. Kamiya and Y. P. Yampolskii, *J. Polym. Sci. Part B: Polym. Phys. Ed.*, **34**, 369–378, Copyright © 1996, John Wiley & Sons, Inc. Reprinted with permission of John Wiley & Sons, Inc. (d) Reproduced by permission of Wiley-VCH from 'The solubility of vinyl chloride in poly(vinyl chloride)', A. R. Berens, *Angew. Makromol. Chemie*, **47**, 97–110 (1975)

tions'' of sorbed species, in local chemical equilibrium with one another, are envisioned – those in long-lived, non-equilibrium free-volume elements and those dissolved in more densely packed regions within polymers. In the low-pressure limit, as $p \longrightarrow 0$, one obtains the infinite

dilution gas solubility coefficient:

$$S = k_D + C'_H b \tag{1.39}$$

which determines the initial slope of the isotherm. At higher pressure, the slope is determined by the Henry's law solubility coefficient, k_D, and the transition between these two sections of the isotherm occurs at $p = 1/b$. At low to moderate pressures, gas sorption in glassy polymers is often dominated by the Langmuir term in Equation (1.38) (i.e. $C'_H b \gg k_D$) [113], especially in polymers with high T_g. The k_D and b parameters are treated as equilibrium constants whose temperature–dependence is given by van't Hoff relationships with negative enthalpies of sorption ΔH_s, (usually, ΔH_s that corresponds to the temperature-dependence of b is more exothermic than that of k_D) [8,62,88]. Both k_D and b values are often correlated with penetrant condensability. For example, k_D and b are presented as a function of gas critical temperatures in Figure 1.12 in a manner consistent with the correlation of total solubility with T_c, as shown in Figure 1.5 [114].

The Langmuir sorption capacity parameter, C'_H, is interpreted as a measure of non-equilibrium or unrelaxed volume in polymers. For CO_2 sorption, this parameter, as determined from analysis of experimental sorption isotherms, is often consistent with the value estimated as follows:

$$C'_H = 22\,414\frac{V_g - V_r}{V_g} \tag{1.40}$$

where V_g is the total specific volume of the polymer, V_r is the total specific volume of the equilibrium liquid or rubbery polymer if vitrification is precluded, and $\rho*$ is the hypothetical density of liquid-like solutes sorbed in Langmuir sites [7,115,116]. The non-equilibrium excess volume providing the locus of the Langmuir sorption derives from the excess volume inherently present in glassy polymers at temperatures below T_g. Figure 1.13 presents the effect of temperature on the density of Ultem® 1000 polyetherimide. As the polymer is cooled from above to below the T_g, there is an abrupt change in the slope of the specific volume versus temperature plot, marking the onset of severe kinetic constraints in the polymer's ability to reorganize itself to attain its equilibrium specific volume, V_r. The material is kinetically trapped in a higher-volume state, V_g. The difference between the observed specific volume and the equilibrium specific volume, $V_g - V_r$, is believed to be the locus of the non-equilibrium excess sorption characterized by the Langmuir capacity parameter, C'_H. According to this interpretation, C'_H should depend upon temperature. It should decrease as temperature increases and vanish when the experimental temperature T

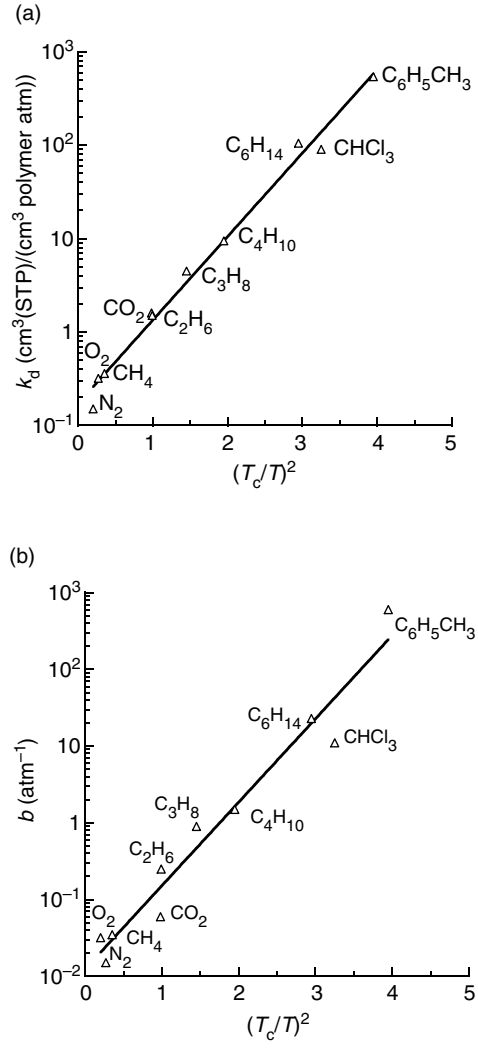


Figure 1.12 Correlation of (a) k_D and (b) b with squared reduced critical temperature in amorphous Teflon AF2400 [114]

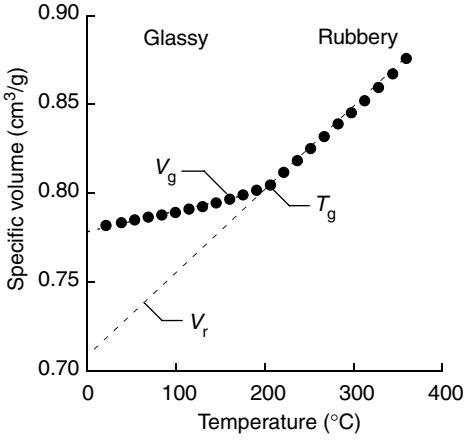


Figure 1.13 Effect of temperature on specific volume in the rubbery and glassy states of Ultem® 1000 polyetherimide at 0 MPa; the data have been extrapolated to 0 MPa from higher pressures [175]. Copyright © 1995 from Standard Pressure, Volume, Temperature Data by P. Zoller and D. J. Walsh. Reproduced by permission of Routledge/Taylor & Francis Group, LLC

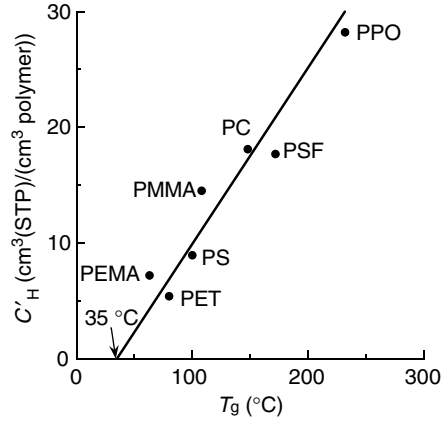


Figure 1.14 Variation of C'_H for carbon dioxide with polymer glass transition temperature. The sorption data used to evaluate C'_H were measured at 35 °C, and the polymers are poly(2,6-dimethyl-1,4-phenylene oxide) (PPO), polysulfone (PSF), polycarbonate (PC), poly-(methyl methacrylate) (PMMA), polystyrene (PS), poly (ethyl methacrylate) (PEMA) and poly(ethylene terephthalate) (PET) [69]. From 'Gas sorption and transport in poly(phenylene oxide) and comparisons with other glassy polymers', K. Toi, G. Morel and D. R. Paul, *J. Appl. Polym. Sci.*, **27**, 2997–3005, Copyright © 1982, John Wiley & Sons, Inc. Reprinted with permission of John Wiley & Sons, Inc.

becomes equal to T_g. Therefore, when considering the sorption properties of a single gas in many different polymers, C'_H should increase as T_g increases. Such behavior is well documented [76,112,115]. Figure 1.14 provides an illustration of this principle. If one considers a variety of gases in a single polymer, for gases below their critical temperature, T_c, the observed C'_H values roughly decrease with increasing molecular size (cf. Figure 1.15) [12,62,114,117]. That is, larger gas molecules sample progressively smaller fractions of available unrelaxed (free) volume in glassy polymers during sorption.

In spite of the intuitive consistency of the dual-mode sorption model, it must be considered an empirical, phenomenological model that fits the experimentally measured isotherms but lacks a molecular foundation. That is, it cannot be used to predict sorption isotherms in the absence of experimental data, and its parameters, including the equilibrium parameters k_D and b, are observed to depend on sample processing history [118,119]. The parameters also depend on the range of pressure explored in sorption measurements, especially when working at higher pressures [120]. Recent efforts have focused on

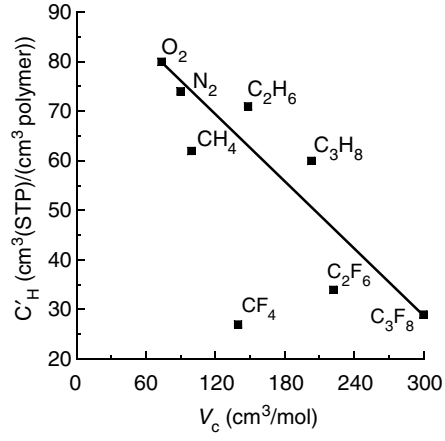


Figure 1.15 The effects of gas molecular size on C'_H in PTMSP at 35 °C [62]. From 'Sorption and transport of hydrocarbon and perfluorocarbon gases in poly(1-trimethylsilyl-1-propyne)', T. C. Merkel, V. Bondar, K. Nagai and B. D. Freeman, *J. Polym. Sci. Part B: Polym. Phys. Ed.*, **37**, 273–296, Copyright © 1999, John Wiley & Sons, Inc. Reprinted with permission of John Wiley & Sons, Inc.

developing sorption models based on applying statistical mechanics concepts to develop equations-of-state for non-equilibrium systems such as glassy polymers. These equations-of-state can then form the foundations of new sorption models that have more predictive ability than the dual-mode model. A review of this approach is presented in Chapter 5.

Sigmoidal-shaped sorption isotherms, such as the one presented in Figure 1.11(d) are often observed in glassy polymers when the solute concentration becomes high enough that Henry's law is no longer adequate for modeling sorption in the equilibrium structure of the polymer. In these cases, the isotherm is often modeled by using a combination of the Langmuir contribution of the dual-mode model and the Flory–Huggins model to replace the Henry's law component of the dual-mode model. Often, in the region where the isotherm becomes convex to the abscissa, the polymer is believed to contain sufficient amounts of penetrant to become plasticized and to have the T_g of the gas–polymer system reduced towards the experimental temperature [121]. It is easiest to observe such isotherms for highly sorbing gases (e.g. CO_2 and organic vapors) and polymers having relatively low glass transition temperatures.

1.3.2 Diffusion

Figure 1.16 presents various examples of the observed dependence of diffusivity on concentration. For low-sorbing permanent gases in polymers, the diffusion coefficients are usually independent of gas concentration in the polymer, as illustrated in Figure 1.16(a) [122]. Plasticization due to sorption of high concentrations of penetrants, such as organic vapors, often result in linear (cf. Figure 1.16(b)) or even exponential increases in D [123–126]. One of the principle explanations of this behavior is that penetrant molecules contribute free volume to a polymer/penetrant mixture when they sorb into it, and the increase in free volume due to penetrant sorption increases the polymer chain mobility and penetrant diffusion coefficients. Clustering is accompanied by an effective increase in the mean size of the diffusing species and is manifested by a decrease in D with increasing concentration (cf. Figure 1.16(c)) [127]. The dependence of D on concentration allows one to distinguish between the two possible mechanisms of sorption isotherms which are convex to the pressure axis: Flory–Huggins behavior is usually accompanied by increases in D, whereas clustering phenomena lead to reduced diffusion coefficients at higher vapor activity and solute concentration. Finally, Figure 1.16(d) is characteristic of diffusion coefficients for many penetrants at relatively low concentrations in glassy polymers, and the line through the data in Figure 1.16(d) represent fits of the transport model based on dual-mode concepts [128].

1.3.3 Permeability

The forms of $S(p)$ and $D(p)$ determine the pressure and concentration behavior of permeability, as shown in Figure 1.17. The permeability of low-sorbing penetrants exhibit little or no change in permeability with increasing pressure, as shown in Figure 1.17(a). However, some penetrants sorb into polymers to such a degree that they plasticize the polymer. Plasticization effectively increases the chain spacing in the polymer and increases the chain mobility so that the diffusion and permeation coefficients increase with increasing penetrant pressure, as shown in Figure 1.17(b). Another situation resulting in permeability increases with increasing upstream pressure can be found in rubbery polymers, such as PDMS; diffusion coeffcients of organic vapors can remain approximately constant (or even decrease slightly) up to even high penetrant concentrations, but if solubility follows the Flory–Huggins model and increases at high penetrant activity, then permeability can also increase strongly with increasing penetrant pressure [106]. In glassy polymers, the dual-mode sorption and mobility model predicts a decrease in permeability with increasing pressure, as exemplified by CO_2 in polycarbonate in Figure 1.17(c) [129]. This trend has been confirmed by many other studies [112]. However, plasticization can occur at higher penetrant concentrations, which often leads to an increase in permeability values at higher pressures, as shown in Figure 1.17(d) [124].

1.3.4 Selectivity

Most of the permeation data reported in the literature were measured by using one gas at a

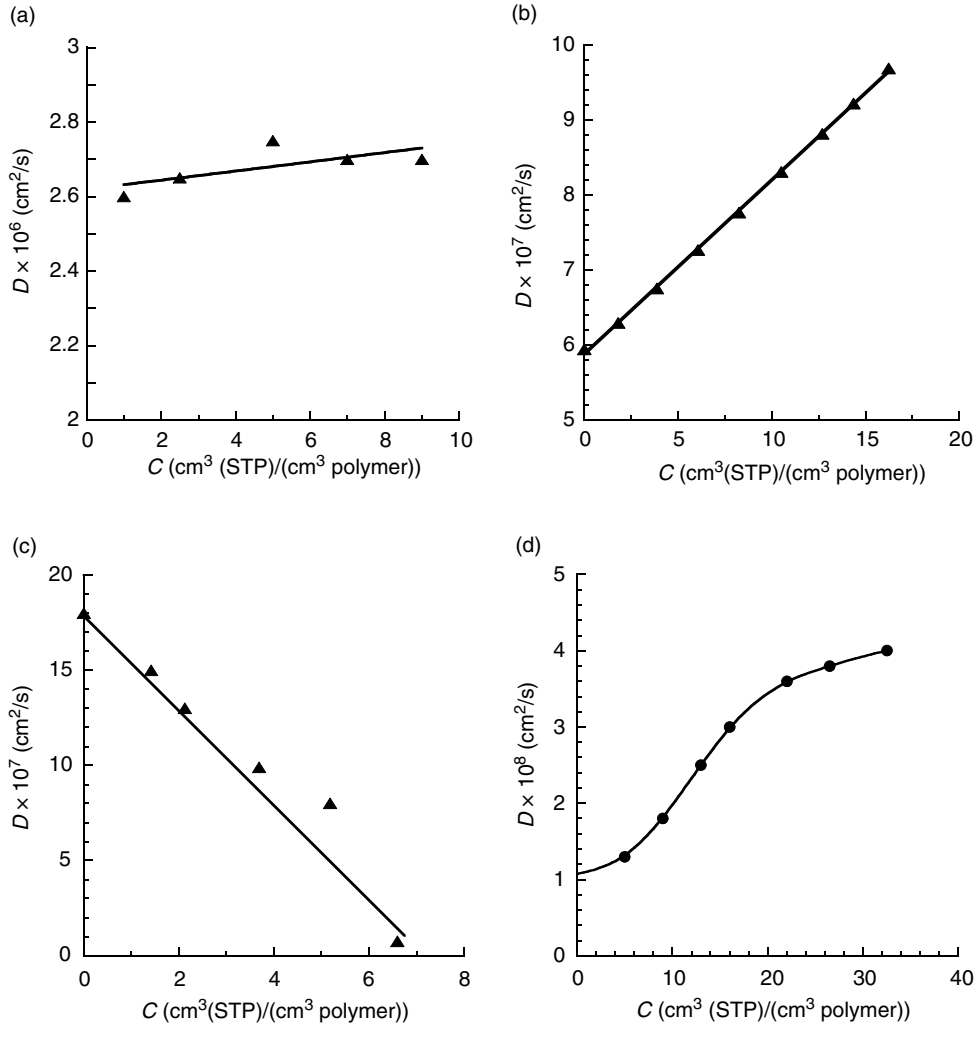


Figure 1.16 Concentration-dependence of diffusion coefficients: (a) low-sorbing gases (O_2 in Teflon AF1600 [122] at 35 °C); (b) plasticization in rubbery polymers (CO_2 in cross-linked poly(ethylene glycol diacrylate) [126] at 35 °C); (c) cluster formation (water in ethylcellulose at 25 °C) [127]); (d) dual-mode behavior in a glassy polymer (CO_2 in polycarbonate at 35 °C [128]). (a) Reprinted with permission from A. Y. Alentiev *et al*., *Macromolecules*, **35**, 9513–9522 (2002). Copyright (2002) American Chemical Society. (b) Reprinted in part with permission from H. Lin and B. D. Freeman, *Macromolecules*, **38**, 8394–8407 (2005). Copyright (2005) American Chemical Society. (c) Reproduced by permission of Wiley-VCH from 'Temperature effects during the sorption and desorption of water vapor in high polymers. I. Fibers, with particular reference to polymers', A. A. Armstrong and V. T. Stannett, *Angew. Makromol. Chemie*, **90**, 145–160 (1966). (d) From 'Carbon dioxide sorption and transport in polycarbonates', *J. Polym. Sci. Part B: Polym. Phys. Ed.*, **14**, 687–702, Copyright © 1976, John Wiley & Sons, Inc. Reprinted with permission of John Wiley & Sons, Inc.

time (i.e. single gas or pure gas measurements). However a key commerical application is the separation of gas mixtures, and so it is of significant interest to understand the transport properties of mixtures of gases in polymers and to understand how they are similar to and different from the pure-gas transport properties. Examples of the most common types of behavior are

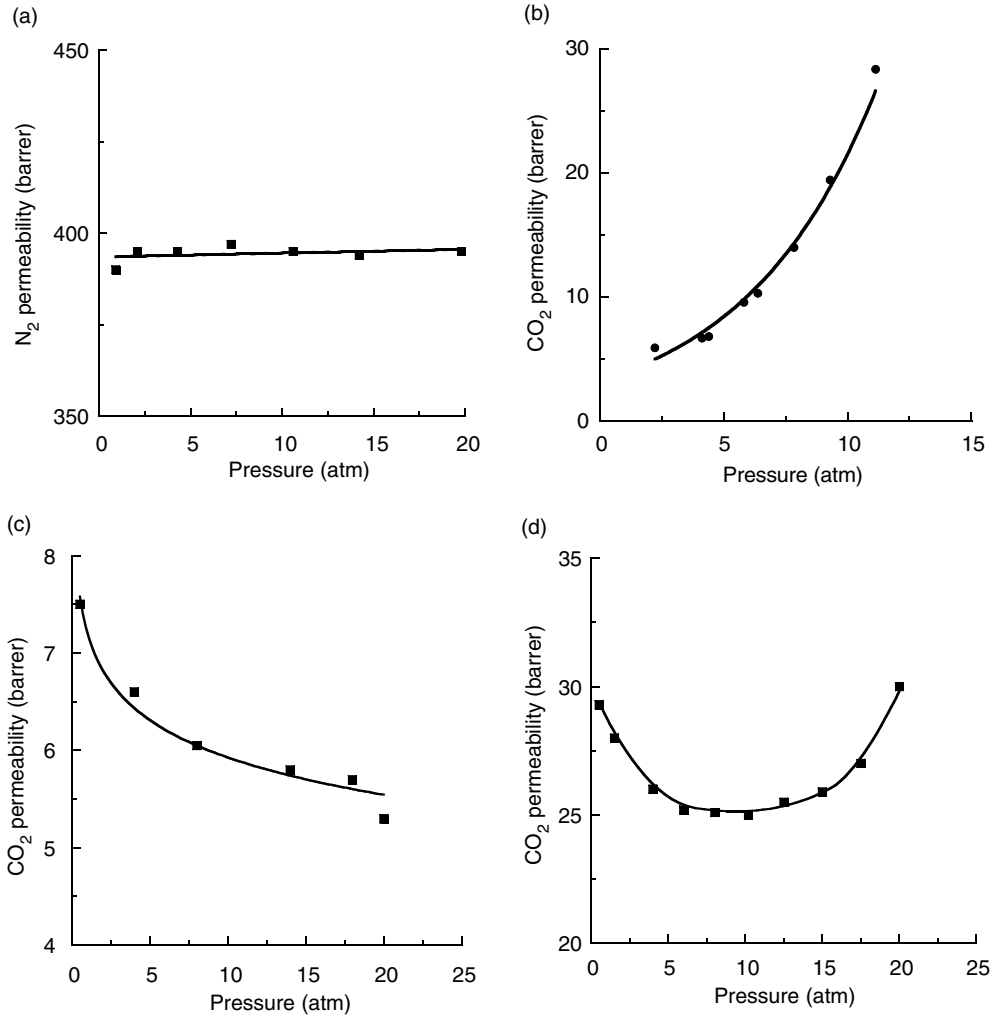


Figure 1.17 Influence of upstream pressure on permeability coefficients: (a) low-sorbing gases (N_2 in PDMS at 35 °C [34]); (b) plasticization of a rubbery polymer (cross-linked poly(ethylene glycol diacrylate) at −20 °C [138]); (c) dual-mode behavior in a glassy polymer (CO_2 in Lexan polycarbonate [129]); (d) dual-mode behavior at low pressure (<10 atm) and plasticization at higher pressure (CO_2 in polytetrabromophenolphthalein at 35 °C [124]). (a) From 'Gas sorption, diffusion and permeation in polydimethylsiloxane', T. C. Merkel, V. Bondar, K. Nagai, B. D. Freeman and I. Pinnau, *J. Polym. Sci. Part B: Polym. Phys. Ed.*, **38**, 415–434, Copyright © 2000, John Wiley & Sons, Inc. Reprinted with permission of John Wiley & Sons, Inc. (b) Reprinted with permission from H. Lin, E. van Wagner, B. D. Freeman, L. G. Toy and P. Ragubir, 'New membrane materials for CO_2/H_2 separation and a model for pure and mixed gas permeability', *Science*, **311**, 639–642 (2006). Copyright (2006) AAAS. (c) From 'Carbon dioxide sorption and transport in polycarbonates', *J. Polym. Sci. Part B: Polym. Phys. Ed.*, **14**, 687–702, Copyright © 1976, John Wiley & Sons, Inc. Reprinted with permission of John Wiley & Sons, Inc. (d) Reprinted in part from R. T. Chern and C. N. Provan, *Macromolecules*, **24**, 2203–2207 (1991). Copyright (1991) American Chemical Society

provided. Mixed-gas selectivity is discussed first, and then examples of mixed-gas permeability are presented.

Often, mixed-gas and pure-gas selectivity values are different. However, there are some examples where this is not the case. For exam-

ple, the mixed- and pure-gas selectivities for rubbery polymers can be equivalent or nearly so. Figure 1.18(a) presents such a case; it involves acetone and nitrogen copermeation in PDMS [106]. In this case, acetone and nitrogen essentially copermeate through PDMS as if they were each the only penetrant in the polymer. That is, the presence of acetone in the polymer does not influence the transport of nitrogen, and vice versa. This pattern of behavior might be classified as ideal, since it implies that one can predict mixture permeation properties based only on pure-gas permeation data. A similar behavior is expected for light gas mixture copermeation through glassy and rubbery polymers (e.g. O_2/N_2 or H_2/N_2 mixture separation by membranes).

A counter-example to the behavior in Figure 1.18(a) is presented in Figure 1.18(b) [130]. In rubbery poly(ethylene glycol diacrylate) (and in many strongly size-sieving glassy polymers as well), the sorption of a more condensable component (CO_2 in this case) apparently decreases the T_g of the polymer [21,131], thereby increasing the free volume available to both CO_2 and CH_4. The most important effect of the increase in free volume is believed to be an increase in gas diffusivity and, in turn, permeability, as expected when based on Equations (1.33) and (1.34). Thus, pure gas CO_2 permeability increases significantly with increasing CO_2 feed pressure; methane (which exhibits much lower sorption than CO_2) has a minimal effect on free volume, and so its permeability is approximately independent of methane feed pressure. As a result, the selectivity estimated based on pure-gas permeability coefficients increases with increasing CO_2 pressure. However, when CO_2 and CH_4 permeabilities are measured in mixture permeation experiments, the selectivity actually decreases with increasing CO_2 partial pressure. This effect may be rationalized by considering the effect of increasing free volume (due to increased CO_2 sorption at higher CO_2 partial pressure) on the diffusivity selectivity:

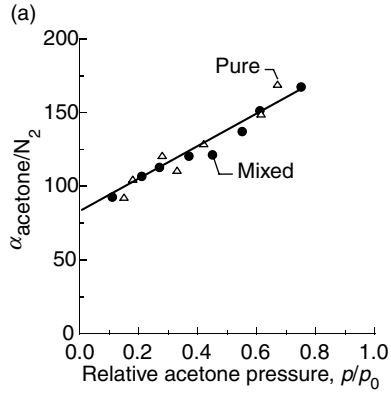
$$\frac{D_{CO_2}}{D_{CH_4}} = \frac{A_{CO_2}}{A_{CH_4}} \exp\left(\frac{B_{CH_4} - B_{CO_2}}{FFV}\right) \tag{1.41}$$

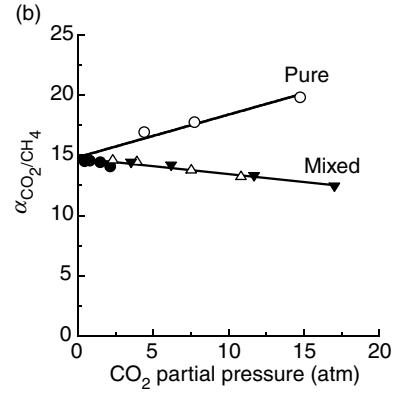
The value of B_{CH_4} is greater than that of B_{CO_2} (cf. Figure 1.10), and so as fractional free volume increases, the diffusivity selectivity (i.e. D_{CO_2}/D_{CH_4}) decreases, and so overall mixture selectivity decreases. That is, increasing free volume reduces the size-sieving ability of the polymer. In other words, as CO_2 partial pressure in the CO_2/CH_4 mixture increases, the diffusivity of CH_4 increases more than that of CO_2, which reduces diffusivity selectivity and overall selectivity.

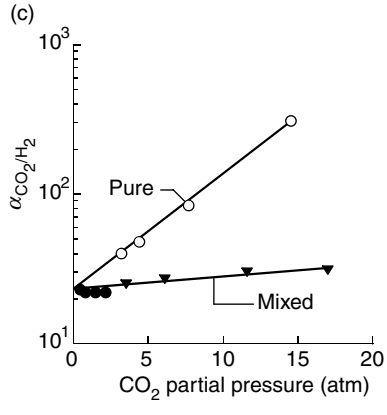
However, reduced size-sieving ability as a result of plasticization by a strongly sorbing component is not necessarily always detrimental to membrane separation performance. Using the same cross-linked rubbery polymer just discussed, separation experiments were performed by using CO_2/H_2 mixtures rather than CO_2/CH_4 mixtures [130]. The results are presented in Figure 1.18(c). The polymer is 'reverse-selective' for this separation. That is, it is more permeable to the larger component (CO_2) than to the smaller component (H_2). Presumably, the solubility selectivity strongly favors CO_2 (the more condensable molecule), and is apparently large enough to more offset than the diffusion selectivity, which would presumably favor H_2, since it is the smaller molecule. As CO_2 partial pressure in the feed gas increases, the CO_2 concentration in the polymer increases, T_g apparently decreases, and FFV apparently increases. As discussed earlier pure gas selectivity increases with increasing CO_2 pressure because CO_2 permeability increases strongly with increasing CO_2 feed pressure (cf. Figure 1.17(b)), and H_2 permeability is essentially independent of H_2 feed pressure. In the mixture, H_2 permeability also increases with increasing CO_2 partial pressure in the feed gas, and so mixture selectivity is lower than pure-gas selectivity. However, CO_2/H_2 mixed-gas selectivity actually increases (from 15 to 18) as CO_2 partial pressure in the feed increases. This observation can be rationalized by considering the effect of free volume on diffusivity selectivity for this 'reverse-selective' case:

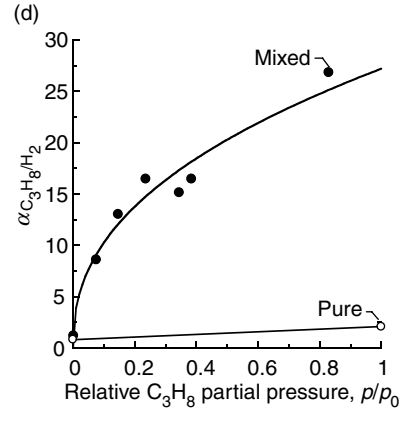
$$\frac{D_{CO_2}}{D_{H_2}} = \frac{A_{CO_2}}{A_{H_2}} \exp\left(\frac{B_{H_2} - B_{CO_2}}{FFV}\right) \tag{1.42}$$

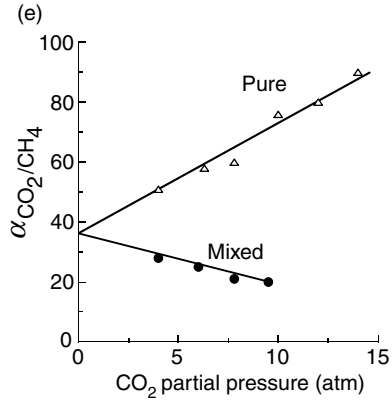
As shown in Figure 1.10, B_{CO_2} is greater than B_{H_2}. Therefore, as FFV increases due to increasing CO_2 sorption at higher CO_2 partial pressures,


(a)
200
150
100
50
0
Pure
Mixed
$\alpha_{acetone/N_2}$
0.0 0.2 0.4 0.6 0.8 1.0
Relative acetone pressure, p/p_0


(b)
25
20
15
10
5
0
Pure
Mixed
α_{CO_2/CH_4}
0 5 10 15 20
CO_2 partial pressure (atm)


(c)
10^3
10^2
10^1
Pure
Mixed
α_{CO_2/H_2}
0 5 10 15 20
CO_2 partial pressure (atm)

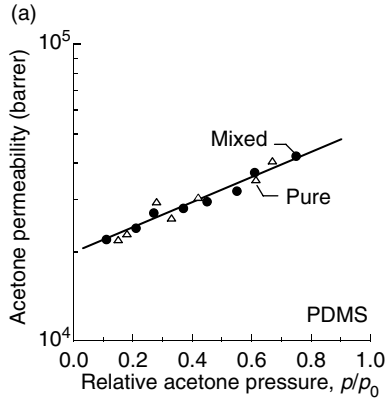

(d)
30
25
20
15
10
5
0
Mixed
Pure
$\alpha_{C_3H_8/H_2}$
0 0.2 0.4 0.6 0.8 1
Relative C_3H_8 partial pressure, p/p_0

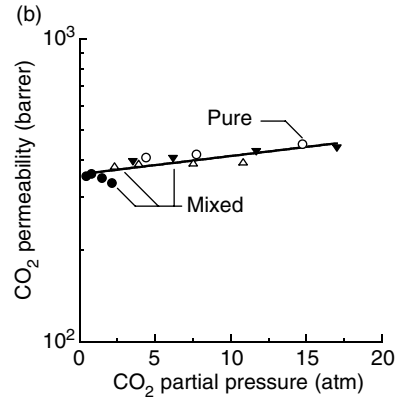

(e)
100
80
60
40
20
0
Pure
Mixed
α_{CO_2/CH_4}
0 5 10 15
CO_2 partial pressure (atm)

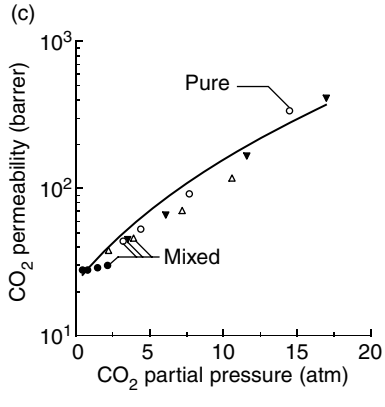
D_{CO_2}/D_{H_2} (which is presumably less than 1 since H_2 is smaller than CO_2) comes closer to 1, which improves overall mixture selectivity. So, in such 'reverse-selective cases' plasticization, which weakens the polymer's size-sieving ability, can be harnessed to simultaneously improve both permeability and selectivity [28]. It should be noted that, because hydrogen sorbs to very low levels, it is very difficult or impossible to measure its solubility in many polymers. Furthermore, there are no mixed-gas sorption data available for mixtures such as CO_2 and H_2, and so the above analysis should be considered as a hypothesis. It is conceivable, although perhaps less likely, that the observed increase in CO_2/H_2 mixed-gas selectivity with increasing CO_2 partial pressure could be due to changes in mixed-gas solubility selectivity. Increases in mixed-gas selectivity with increasing partial pressures of strongly sorbing components (i.e. higher hydrocarbons) in the feed stream have also been reported for PDMS [132].

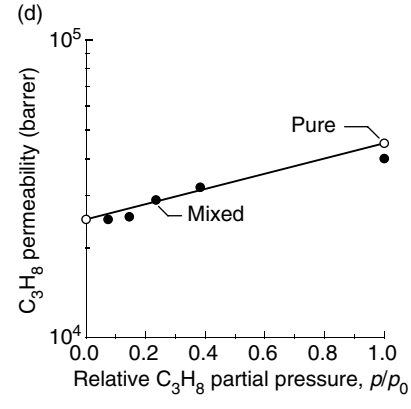
As shown in Figure 1.18(d), the mixed-gas selectivity in 'solubility-selective' (i.e. 'reverse-selective') glassy polymers such as PTMSP can reach high values due to the preferential sorption of the more condensable penetrant in the free volume of the polymer, which blocks the transport of the less condensable penetrant [78]. In this case, selectivity increases strongly with increasing partial pressure of the more condensable component in the feed gas stream, similar to the case just discussed. However, the mechanism for the observed increase in selectivity could be quite different from that in the rubbery polymers (i.e. Figure 1.18(c)), since materials such as PTMSP have large amounts of non-equilibrium excess free volume while rubbers, as equilibrium materials, do not have, and this excess free volume is believed to be the locus of most of the transport in such materials. To date, there are no mixture-sorption studies in such materials which would allow one to understand if the change in selectivity is due to changes in solubility selectivity or changes in diffusivity selectivity [62,133]. Because the transport properties of organic vapor/light gas mixtures in PTMSP often resembles that of selective surface flow in microporous materials such as microporous carbon [134], there are some interpretations of

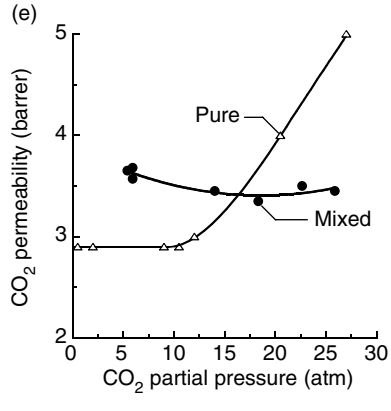
Figure 1.18 Comparison of pure- and mixed-gas selectivities for: (a) acetone/N_2 in PDMS at 28 °C, with feed-gas mixture total pressures ranging from 10 to 12 atm and a permeate pressure at atmospheric [106]; (b) CO_2/CH_4 in cross-linked poly(ethylene glycol diacrylate) (XLPEO) at 35 °C feed-gas mixtures of 10:90 (●), 50:50 (▲), and 80:20 (▼) (mol:mol) CO_2:CH_4 in XLPEO with feed-gas mixture total pressures ranging from 0 to 17 atm and a permeate pressure at atmospheric [130]; (c) CO_2/H_2 in cross-linked XLPEO at −20 °C feed-gas mixtures of 10:90 (●), 50:50 (▲), and 80:20 (▼) (mol:mol) CO_2:H_2 in XLPEO with feed-gas mixture total pressures ranging from 0 to 17 atm and a permeate pressure at atmospheric [138]; (d) C_3H_8/H_2 in PTMSP at 25 °C feed-gas mixture total pressure of 13.7 atm and a permeate pressure at atmospheric [78]; (e) CO_2/CH_4 in cellulose acetate, with feed-gas mixture total pressures ranging from 15 to 47 atm and a permeate pressure at atmospheric [136]. In these examples, acetone, CO_2, and C_3H_8 exhibit significant changes in pure-gas permeability with increasing values of their partial pressure in the feed gas. In contrast, the other components (H_2, N_2 and CH_4) exhibit little or no change in permeability with feed pressure over the ranges of pressure considered in these examples. Therefore, the pure-gas selectivity values were calculated as the pure-gas permeability of the 'more-pressure-dependant component' at a feed pressure equal to the partial pressure of that component indicated on the abscissa, divided by the average permeability of the 'less-pressure-sensitive component' (i.e. N_2 CH_4, and H_2). (a) From 'Pure and mixed gas acetone/nitrogen permeation properties of polydimethylsiloxane', A. Singh, B. D. Freeman and I. Pinnau, *J. Polym. Sci. Part B: Polym. Phys. Ed.*, **36**, 289–301, Copyright © 1998, John Wiley & Sons, Inc. Reprinted with permission of John Wiley & Sons, Inc. (b) Reproduced by permission of Wiley-VCH from 'High performance polymer membranes for natural-gas sweetening', H. Lin, E. van Wagner, B. D. Freeman and I. Roman, *Adv. Mater*, **18**, 39–44 (2006). (c) Reprinted with permission from H. Lin, E. van Wagner, B. D. Freeman, L. G. Toy and P. Ragubir, New membrane materials for CO_2/H_2 separation and a model for pure and mixed gas permeability, *Science*, **311**, 639–642 (2006). Copyright (2006) AAAS. (d) From 'Hydrocarbon/hydrogen mixed gas permeation in poly(1-trimethylsilyl-1-propyne) (PTMSP), poly(1-phenyl-1-propyne) (PPP) and PTMSP/PPP blends', I. Pinnau, C. G. Casillas, A. Morisato and B. D. Freeman, *J. Polym. Sci. Part B: Polym. Phys. Ed.*, **34**, 2613–2621, Copyright © 1996, John Wiley & Sons, Inc. Reprinted with permission of John Wiley & Sons, Inc. (e) From 'Effect of gas composition and pressure on permeation through cellulose acetate membranes', S. Y. Lee, B. S. Minhas and M. D. Donohue, *AIChE Symposium Series No. 261*, Vol. 84, K. Sirkar and D. Lioyd (Eds), pp. 93–101 (1988). Reproduced with permission. Copyright © 1988 AIChE


(a)
Acetone permeability (barrer)
10^5
10^4
Mixed
Pure
PDMS
0.0 0.2 0.4 0.6 0.8 1.0
Relative acetone pressure, p/p_0


(b)
CO_2 permeability (barrer)
10^3
10^2
Pure
Mixed
0 5 10 15 20
CO_2 partial pressure (atm)


(c)
CO_2 permeability (barrer)
10^3
10^2
10^1
Pure
Mixed
0 5 10 15 20
CO_2 partial pressure (atm)


(d)
C_3H_8 permeability (barrer)
10^5
10^4
Pure
Mixed
0.0 0.2 0.4 0.6 0.8 1.0
Relative C_3H_8 partial pressure, p/p_0


(e)
CO_2 permeability (barrer)
5
4
3
2
Pure
Mixed
0 5 10 15 20 25 30
CO_2 partial pressure (atm)

PTMSP transport properties based qualitatively at least, on this concept [133,135].

Conventional, size-sieving glassy polymers generally have a much lower mixed-gas selectivity than pure-gas selectivity due to plasticization, as shown in Figure 1.18(e) for CO_2/CH_4 permeation in cellulose acetate [136]. Other examples of this behavior are available in the literature [123,137]. In such cases, the presence of the more condensable component (CO_2 in this case) is assumed to plasticize the polymer matrix and decrease the diffusivity selectivity, which decreases the permeability selectivity, as explained in detail for the data presented in Figure 1.18(b). However, there are no mixed-gas diffusion and sorption data available to confirm this hypothesis.

Figure 1.19 presents the pure- and mixed-gas permeabilities for the more permeable penetrants in Figures 1.18(a)–1.18(c). For the rubbery polymers (Figures 1.19(a)–1.19(c)), the permeability of the more permeable component increases with increasing partial pressure of this component in the feed. However, the reasons for this behavior are somewhat different. In the case of PDMS, the increase in acetone permeability with increasing acetone feed pressure is due solely to the increase in acetone solubility with increasing acetone feed pressure; acetone diffusivity actually decreases slightly with increasing acetone feed pressure [106]. However, for poly (ethylene glycol diacrylate), the increase in CO_2 permeability (cf. Figures 1.19(b) and 1.19(c)) is due mainly to an increase in CO_2 diffusion coefficient as the CO_2 content in the polymer increases [130,138]. In this sense, the presence of the more soluble (and more permeable) component in poly(ethylene glycol diacrylate) appears to have more influence on the polymer properties (e.g. T_g) than in the case of PDMS and, consequently, the permeation properties of the less soluble species (H_2 and CH_4) are strongly affected by the presence of CO_2 in poly(ethylene glycol diacrylate), whereas nitrogen permeability is essentially unaffected by the presence of even rather high levels of acetone in PDMS. The fundamental basis for this difference in behavior in these rubbery polymers remains an open question. Figure 1.19(d) shows that the permeability of propane in PTMSP is hardly influenced by propane feed pressure, and so the strong increase in propane/hydrogen selectivity shown in Figure 1.19(d) is due essentially entirely to the decrease in H_2 permeability with increasing C_3H_8 partial pressure in the feed. The final case, CO_2 in cellulose acetate, is interesting because, as CO_2 partial pressure in the feed gas mixture increases, CO_2 permeability in the mixture is

Figure 1.19 Comparison of pure- and mixed-gas permeabilities for: (a) acetone in acetone/N_2 mixtures in PDMS at 28 °C, with feed-gas mixtures total pressures ranging from 10 to 12 atm and a permeate pressure at atmospheric [106]; (b) CO_2 in CO_2/CH_4 mixtures in poly(ethylene glycol diacrylate) (XLPEO) at 35 °C feed-gas mixtures of 10:90 (●), 50:50 (Δ), and 80:20 (▼) (mol:mol) CO_2:CH_4 with feed-gas mixtures total pressures total ranging from 0 to 17 atm and a permeate pressure at atmospheric [130]; (c) CO_2 in CO_2/H_2 mixtures in XLPEO at −20 °C feed-gas mixtures of 10:90 (●), 50:50 (Δ) and 80:20 (▼) (mol:mol) CO_2:H_2 with feed-gas mixture total pressures ranging from 0 to 17 atm and a permeate pressure at atmospheric [138]; (d) C_3H_8 in C_3H_8/H_2 mixtures in PTMSP at 25 °C feed-gas pressure of 13.7 atm absolute pressure and a permeate pressure at atmospheric [78]; (e) CO_2 in CO_2/CH_4 in cellulose acetate at 35 °C, with feed-gas mixture total pressures ranging from 0 to 30 atm and a permeate pressure at atmospheric. The mixed gas composition was 46.1 mol% CO_2 [139]. (a) From 'Pure and mixed gas acetone/nitrogen permeation properties of polydimethylsiloxane', A. Singh, B. D. Freeman and I. Pinnau, *J. Polym. Sci. Part B: Polym. Phys. Ed.*, **36**, 289–301, Copyright © 1998, John Wiley & Sons, Inc. Reprinted with permission of John Wiley & Sons, Inc. (b) Reproduced by permission of Wiley-VCH from 'High performance polymer membranes for natural-gas sweetening', H. Lin, E. van Wagner, B. D. Freeman and I. Roman, *Adv. Mater*, **18**, 39–44 (2006). (c) Reprinted with permission from H. Lin, E. van Wagner, B. D. Freeman, L. G. Toy and P. Ragubir, 'New membrane materials for CO_2/H_2 separation and a model for pure and mixed gas permeability', *Science*, **311**, 639–642 (2006). Copyright (2006) AAAS. (d) From 'Hydrocarbon/hydrogen mixed gas permeation in poly(1-trimethylsilyl-1-propyne) (PTMSP), poly(1-phenyl-1-propyne) (PPP) and PTMSP/PPP blends', I. Pinnau, C. G. Casillas, A. Morisato and B. D. Freeman, *J. Polym. Sci. Part B: Polym. Phys. Ed.*, **34**, 2613–2621, Copyright © 1996, John Wiley & Sons, Inc. Reprinted with permission of John Wiley & Sons, Inc. (e) From 'Permeability of dense (homogeneous) cellulose acetate membranes to methane, carbon dioxide and their mixtures at elevated pressures', A. Y. Houde, B. Krishnakumar, S. G. Charati and S. A. Stern, *J. Appl. Polym. Sci.,* **62**, 2181–2192, Copyright © 1996, John Wiley & Sons, Inc. Reprinted with permission of John Wiley & Sons, Inc.

hardly affected, even though selectivity (cf. Figure 1.19(e)) is strongly affected [139]. Additionally, cellulose acetate, which is a glassy polymer, is known to be sensitive to its prior history of exposure to strongly sorbing gases such as CO_2. This sensitivity to history may explain, in part, why the pre- and mixed-gas data do not exhibit the same CO_2 permeability at very low CO_2 partial pressure. Such mixed-gas data are not widely available, and so it is not known to what extent the examples presented here are relevant to other gas mixtures and other polymers. This area could be a very fruitful one for future experimental and modeling studies.

1.4 Effect of Temperature on Transport Parameters

The temperature-dependence of the transport parameters is typically described by Arrhenius–van't Hoff equations [7]:

$$D = D_0 e^{-E_D/RT} \tag{1.43}$$

$$P = P_0 e^{-E_P/RT} \tag{1.44}$$

and Equation (1.25) for solubility. In the equations above, E_D and E_P are the activation energies of diffusion and permeation, respectively. From Equation (1.25), ΔH_s is the enthalpy of sorption, and $E_P = E_D + \Delta H_s$; E_D is always positive, whereas the sign of E_P depends on the relative magnitudes of E_D and ΔH_s. For strongly size-sieving gas separation polymers, such as those used for air separation and H_2 removal from mixtures with hydrocarbons, $E_D > |\Delta H_s|$, and so the resulting values of E_P are positive and permeability increases as temperature increases. However, E_P can be negative in vapor separation applications, such as the removal of volatile organic compounds from air or other light gases using membrane materials such as PDMS [140] and PTMSP, where ΔH_s values exhibit large absolute values or in polymers with very low energy barriers for diffusion (i.e. small E_D values). While E_P and E_D values are typically independent of temperature for transport in glassy polymers, these activation energies can be temperature-dependent in rubbery polymers [36]. A marked break in the Arrhenius behavior is observed in most cases when the measurement temperature passes through T_g [141].

The parameters of the Arrhenius equations (1.43) and (1.44) are strongly interrelated due to the so-called compensation effect – larger preexponential factors correspond to higher activation energies and vice versa [61,142]. For rubbers, van Amerongen observed the following correlation [143]:

$$\ln D_0 = a(E_D/R) - b \tag{1.45}$$

where a and b are constants. For a variety of gases and rubbery polymers, a recent study by Prabhakar *et al.* has shown an apparent universal value of a of $0.002\ K^{-1}$ [144], which was very close to the value proposed by van Amerongen ($0.0023\ K^{-1}$) more than 50 years ago [143]; van Amerongen proposed a universal value of 9.7 for b (when D_0 has units of cm^2/s) [143]. However, Prabhakar *et al.* found that the best single value for b, describing a wide range of data in rubbery polymers, was 8.3 [144]. The agreement between the experimental data and the linear free energy relation for a variety of polymers was more successful if b was allowed to vary from 7.6 to 10.6, depending on the penetrant and the polymer [145]. While there may not be a single, universal value of b, it appears that b values in this narrow range describe the linear free energy relationship for many rubbery polymers and gases. A similar relation has also been observed in glassy polymers [146]. Such equations enable activation energies to be estimated when the D or P values are known at a single temperature; hence, the values of D and P at different temperatures can be estimated from an observation at a single temperature.

As shown in Figure 1.19, E_D is a strong function of the molecular size of the penetrants. A simple interpretation of this phenomenon was given by Meares [40]:

$$E_D = 0.25\, N_0 \pi d^2 \lambda \mathrm{CED} \tag{1.46}$$

where N_0 is the Avogadro constant, d is the kinetic cross-sectional area of a diffusant, CED is the polymer cohesive energy density, and λ is the diffusion jump length, which is usually treated as an adjustable parameter. This equation rationalizes the dependence of E_D on d^2 (Figure 1.20), which then leads to the decrease in gas diffusivity with increasing size (Figure 1.3). However, Equation

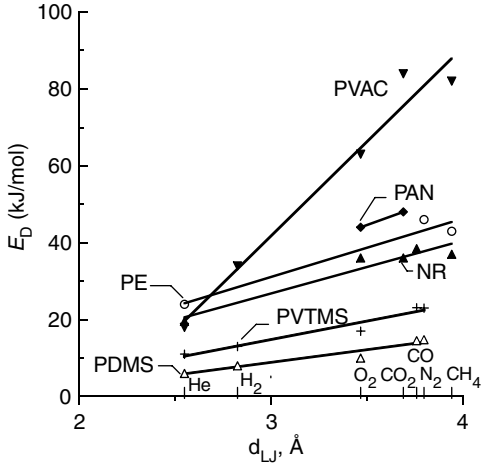


Figure 1.20 Effect of penetrant size on activation energy of diffusion in poly(vinyl acetate) (PVAC) (▼), polyacrylonitrile (PAN) (◆), polyethylene (PE) (○), natural rubber (NR) (▲), PVTMS (+) and PDMS (▲) [103]

(1.46) is not predictive, because the λ values are not known a priori. Analysis of the Meares equation (Equation (1.46)), in conjunction with data from positron annihilation lifetime spectroscopy on the size and concentration of free-volume elements in polymers indicates that the diffusion jump length λ is close to the average distance between adjacent free-volume elements in glassy polymers [105].

Traditionally, the temperature-dependence of D and activation energy, E_D, are interpreted based on transition-state theory [147]. However, activation energies E_D and E_P also correlate with free volume. Polymers with large free volume usually exhibit fairly low activation energies and vice versa [146]. Thus, these two theoretical approaches (free volume and activated-state theory) must be very strongly related because each can provide a rational explanation of much of the available experimental data. Recently, Lin and Freeman have pursued this line of reasoning and have developed the following relation between the activation energy of diffusion and fractional free volume [101]:

$$E_D = \frac{A + b - \left(\frac{B}{FFV}\right)}{\left(\frac{a}{R} - \frac{1}{RT}\right)} \tag{1.47}$$

where A and B are from the free-volume model of diffusion (Equation (1.33)), and a and b are constants from the linear free-energy relation (i.e. Equation (1.45)). It is rather straightforward to build an appropriate concentration-dependence into FFV (and, by extension, into E_D) by allowing FFV to depend on the difference between the experiment temperature and the T_g, and allowing T_g to vary with penetrant concentration using, for example, Chow's model [131], which can be implemented with no adjustable parameters. Because FFV depends on temperature and penetrant concentration, this approach allows E_D to depend in a systematic and consistent fashion on these variables as well. Furthermore, for the series of cross-linked rubbers that Lin *et al.* considered, the following relation was observed for B [101]:

$$B = B_1 + B_2 d_{LJ}^2 \tag{1.48}$$

where B_1 and B_2 are adjustable constants, and d_{LJ} is the Lennard–Jones diameter of the penetrants. This result is consistent with the Meares model scaling of E_D with the square of the penetrant diameter. While the model of Lin *et al.* has not been tested on a wide variety of polymers, it provides a reasonable first step towards integrating the free volume and activated state approaches to describe small molecule transport in polymers. It also provides an indication that these two theoretical viewpoints (i.e. activated state and free volume) are quite probably two equivalent ways of interpreting gas and vapor diffusion in polymers.

1.5 Structure/Property Relations

All physico-chemical properties of polymers depend upon the chemical structure of the polymer repeat units. It is possible to consider directly the chemical structure effects of linear polymers on their transport properties. The manifestation of these effects is different for polymers above and below their glass transitions.

As has been mentioned, permeability and diffusion coefficients in rubbers are strongly influenced by their glass transition temperatures, and T_g values are sensitive to the main- and side-chain structure of elastomers. Table 1.4 illustrates the effect of side-chains on T_g and permeability

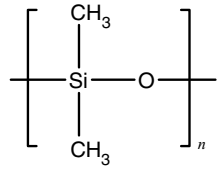
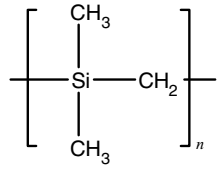
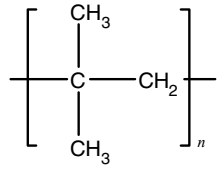
Table 1.4 Permeability of siloxane polymers, $[Si(CH_3)-O]_n$, at 35 °C. From 'Structure–permeability relationship in silicone polymers', S. A. Stern, V. M. Shah and B. J. Hardy, *J. Polym. Sci. Part B. Polym. Phys. Ed.*, **25**, 1263–1298, Copyright © 1987, John Wiley & Sons, Inc. Reprinted with permission of John Wiley & Sons, Inc.

		P (barrer) [148]		
R	T_g (K)	O_2	CH_4	C_3H_8
CH_3	150	930	1350	18 000
n-C_3H_7	153	380	570	9 000
n-C_8H_{17}	181	190	310	5 600
C_6H_5	245	32	36	480

of polysiloxanes. As the silicon atom substituents become larger, glass transition temperature increases, and permeability coefficients decrease [148]. It is also interesting to follow the changes of the properties when the structure of the main-chain is changed in a systematic manner. As shown in Table 1.5, chain flexibility is reduced when the oxygen atom in siloxane is replaced by a methylene group, as is indicated by the increase in T_g and reduction in permeability. Further decreases in permeability by virtue of reduced main-chain flexibility can be observed for polyisobutylene, where the silicon atom is replaced by carbon.

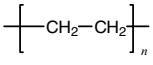
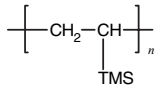
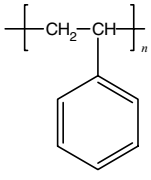
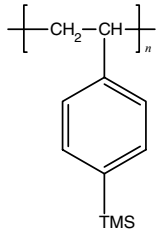
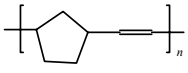
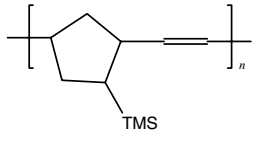
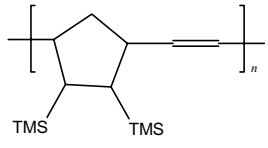
The repeat unit chemical structure also influences gas permeability in glassy polymers. Abundant data on this subject can be found in numerous reviews [23,64,83,84,149–151]. For example, striking effects are produced by introducing bulky $Si(CH_3)_3$ groups into various main-chains. Thus, in vinylic polymers, replacement of small polar CN groups in polyacrylonitrile by this group to form poly(vinyltrimethyl silane) results in an increase in oxygen permeability from 0.0005 to 44 Barrer [37,38,152], a change of nearly five orders of magnitude. The effect on permeability of introducing trimethylsilyl (TMS) groups into various polymers is illustrated in Table 1.6 [153–156]. Permeability increases in all cases upon introduction of $Si(CH_3)_3$ groups

Table 1.5 Glass transition temperatures and permeabilities of a systematic series of elastomers

			P (barrer)[a]		
Polymer	Structure	T_g (K)	He	CH_4	CO_2
Polydimethylsiloxane [148]		150	560	1350	4500
Polydimethylsilylmethylene [148]		185	98	130	550
Polyisobutylene [36]		199	8.4	—	5.2

[a]Permeability data for polydimethylsiloxane and polydimethylsilylmethylene are at 35 °C, a feed pressure of 9 atm, and atmospheric permeate pressure; permeability data for polyisobutylene are at 25 °C and a pressure range in which the permeability is constant.

Table 1.6 The effect of introduction of trimethylsilyl (i.e. $Si(CH_3)_3$ (TMS)) groups into polymers on the gas transport properties [153–156]

Polymer	Modified polymer	Polymer P_{O_2} (barrer)[a]	Polymer α_{O_2/N_2}	Modified polymer P_{O_2} (barrer)[a]	Modified polymer α_{O_2/N_2}
		2.9	3.0	44	4.3
		1.2	5.5	14	3.3
		2.8	1.7	30	3.8
		2.8	1.7	95	3.8

[a]Permeability measurements were performed at 22 °C and at low pressure.

and often without changing selectivity. Extensive studies of glassy polymers indicate that TMS groups lead to increases in both diffusion and solubility coefficients due to an enhancement in polymer free volume [153].

In glassy polymers, increasing the size of side-groups often, but not always, increases free volume and gas permeability. Detailed studies of polyacetylenes of varying structures [84] showed that: (i) certain sizes and shapes of side-groups most efficiently disrupt chain packing (thereby increasing gas permeability) and (ii) symmetry of side-groups contributes to greater gas permeability (cf. Table 1.7). More detailed considerations of these issues and the structure-dependence of transport properties of polyacetylenes are found in Chapter 9.

In densely packed materials, like aromatic polycarbonates, substitution of hydrogen atoms on aromatic rings by methyl groups or other large substituents can disrupt chain packing, which leads to marked increases in gas permeability, as shown by the experimental data in Table 1.8 [157]. The methyl substitution reduced both chain motion and packing as indicated by the T_g and FFV changes [157]. Substitution of halogens (i.e. Cl, Br) introduces additional polar groups into the polymer, which caused T_g and T_γ to increase significantly, indicating reductions in chain mobility. The halogen substitution also reduced FFV. The more efficient chain packing and loss of chain mobility in the halogen tetrasubstituted polycarbonates lowered CO_2 and CH_4 permeability. These systematic studies of gas transport properties in polycarbonates were driven, in part, by the commercial use of substituted polycarbonates as gas separation membrane materials by the Dow Chemical Company and later by Generon, which was 'spun off' from Dow's gas separation membrane effort.

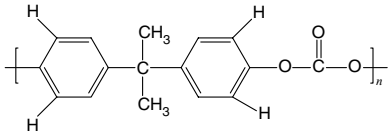
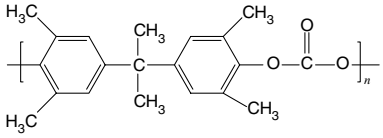
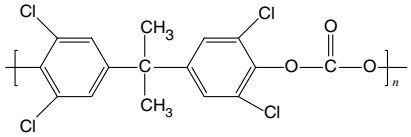
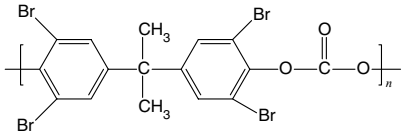
Table 1.7 Effect of substituent size and symmetry on permeability and selectivity in substituted acetylene polymers $+CMe{=}CR+_n$ [84]. Reprinted from *Progress in Polymer Science*, **26**, K. Nagai, T. Masuda, T. Nakagawa, B. D. Freeman and I. Pinnau, 'Poly[1-(trimethylsilyl)-1-propyne] and related polymers: synthesis, properties and functions', 721–798, Copyright (2001), with permission from Elsevier

R	P_{O_2} (barrer)[a]	α_{O_2/N_2}
$SiMe_3$	6000	1.8
$GeMe_3$	1800	1.5
$SiMe_2Et$	970	2.0
$SiEt_3$	860	2.0
$SiMe_2Pr$	100	2.8
$SiMe_2CH_2SiMe_3$	75	3.6

[a]Permeability data are reported at 25 °C.

Because polysulfone has been used for quite some time by Air Products (through their Permea division) as a commercial gas separation membrane material, there have been many studies of its permeation properties [158–160] and attempts to modify it chemically to improve its gas transport properties [161–163]. Table 1.9 presents data for polysulfone and a few variants that have similar modifications as those presented in Table 1.8 for the polycarbonates. In this regard, tetramethyl substitution of polysulfone, to produce TMPSF, has a similar effect on the gas transport properties of polysulfone and polycarbonate; CO_2 permeability increases strongly and CO_2/CH_4 selectivity remains essentially constant relative to values for the unsubstituted polymer [161]. The tetramethyl substituted material has significantly higher T_g and higher free volume. That is, placing the four methyl substituents symmetrically on the aromatic rings stiffens the chain backbone and increases the free volume of the polymer. Higher free volume leads to higher permeability, and the stiffer chain backbone

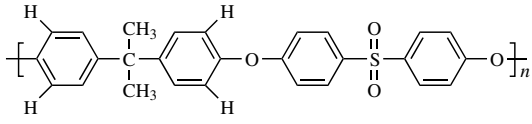
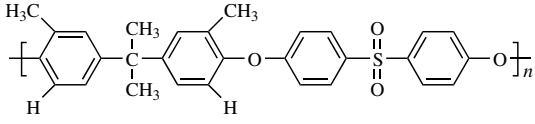
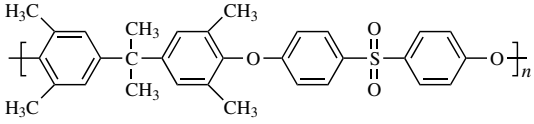
Table 1.8 Physical, thermal and transport properties of substituted polycarbonates [76,157]. From 'Gas sorption and transport in substituted polycarbonates', N. Muruganandam, W. J. Koros and D. R. Paul, *J. Polym. Sci. Part B*: *Polym. Phys. Ed.*, **25**, 1999–2026, Copyright © 1987, John Wiley & Sons, Inc. Reprinted with permission of John Wiley & Sons, Inc.

Polymer	FFV[a]	T_g (°C)	T_γ (°C)	P_{CO_2} (barrer)[b]	α_{CO_2/CH_4}
	0.164	150	−100	6.0	23.3
	0.180	193	50	17.6	22.0
	0.179	230	112	6.7	29.7
	0.133	263	120	4.2	33.6

[a]Density measurements were conducted at 30 °C [76].

[b]Permeability measurements were conducted at 35 °C, 20 atm feed pressure and a permeate pressure 'at vacuum'.

Table 1.9 Physical, thermal and transport properties of substituted polysulfones [161]. Reprinted from *Polymer*, **32**, J. S. McHattie, W. J. Koros and D. R. Paul, 'Gas transport properties of polysulfones. 1. Role of symmetry of methyl group placement on bisphenol', 840–850, Copyright (1991), with permission from Elsevier

Polymer	FFV	T_g (°C)	P_{CO_2} (barrer)[a]	α_{CO_2/CH_4}
	0.156	186	5.6	22
	0.149	180	2.1	30
	0.171	242	21	22

[a]Permeability measurements were conducted at 35 °C, 10 atm feed pressure and a permeate pressure 'at vacuum'.

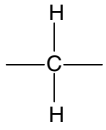
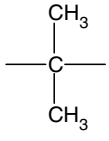
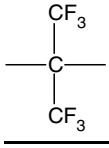
mitigates losses in selectivity that would typically accompany an increase in free volume. In contrast, dimethyl substitution (DMPSF) significantly lowers CO_2 permeability and increases CO_2/CH_4 selectivity relative to that of either polysulfone or TMPSF [161]. FFV in DMPSF is lower than that in polysulfone. This reduction in free volume has been ascribed to more efficient chain packing in the dimethyl substituent than in the unsubstituted analog. Based on dynamic mechanical thermal analysis studies, local segmental mobility in dimethyl-substituted PSF is markedly more constrained than in PSF, and this decrease in local segmental mobility is probably linked to the decrease in free volume and the observed changes in properties. The dimethyl substitution of the aromatic rings may strongly decrease the ability of the phenyl rings to undergo segmental rotation, resulting in a greater tendency for the polymer chains to pack efficiently [161,164].

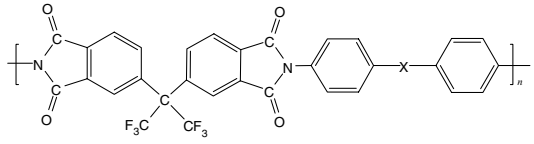
As the preceding text suggests, many chemical structural variations have been pursued in an attempt to produce polymers with better gas separation properties. A few of the more widely studied effects are mentioned in the text that follows, and illustrative examples of the effect of these variables on transport properties are provided.

1.5.1 Connector Groups

Gas transport properties are influenced by the polymer connector groups due to the effect of these groups on chain mobility and chain packing. T_g and FFV are macroscopic characteristics of polymer chain mobility and packing. Linkages that have low energy barriers for intersegmental bond rotations, such as $-O-$ and $-CH_2-$, typically facilitate torsional movement within the polymer backbone, which reduces the chain stiffness, and, in turn, the polymer T_g [165]. By increasing the torsional movement of polymer segments, and thus reducing T_g, penetrant diffusion coefficients often increase. However, bulky groups that stiffen the chain backbone and increase T_g, which tends to decrease diffusion coefficients, can also introduce additional free volume into the polymer matrix, which tends to increase diffusion coefficients. So, it is not unusual that the introduction of non-polar, large groups increases both T_g and gas diffusion coefficients simultaneously. This situation is illustrated in the family of polyimides shown in Table 1.10 [165,166]. Both T_g and FFV increase as more and more bulky connector groups are introduced into the polymers [165]. The diffusion coefficient and permeability increase as T_g increases due to the enhancement in FFV.

Table 1.10 The effect of connector group type on physical properties and gas transport characteristics in a systematic series of aromatic polyimides[a,b] [165,166]. Reprinted from *Journal of Membrane Science*, **50**, M. R. Coleman and W. J. Koros, 'Isomeric polyimides based on fluorinated dianhydrides and diamines for gas separation applications', 285–297, Copyright (1990), with permission from Elsevier

×	T_g (°C)	FFV	P_{CO_2} (barrer)	α_{CO_2/CH_4}	$D_{CO_2} \times 10^8$ (cm^2/s)	S_{CO_2} (cm^3 (STP)/(cm^3 atm)
—O—	304	0.164	23	60.5	3.6	4.89
	304	0.160	19.3	44.9	3.7	3.96
	310	0.168	30	42.9	5.4	4.24
	320	0.190	63.9	39.9	10	4.72

[a]General structure: 

[b]Experiments were conducted at 35 °C and a feed pressure of 10 atm.

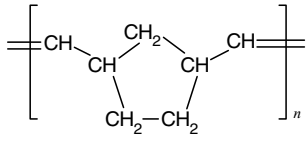
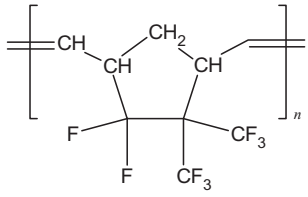
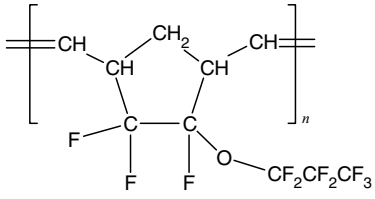
1.5.2 CF_3 and Other Fluorinated Moieties as Side-chains

Generally, $-C(CF_3)_2$ groups have been added to aromatic polymers, such as polyimides and polycarbonates, to disrupt chain packing (i.e. increase free volume). However, $-C(CF_3)_2$ moieties also affect chain packing and overall gas transport differently when added as a side-chain [167]. As shown in Table 1.11, in polynorbornenes containing fluorinated side-chains, the permeability enhancement is mainly due to increases in solubility and, depending on the side-chain, on changes in diffusion coefficients to a lesser extent. The change in solubility has been attributed to the change in T_g with fluorinated side-groups, which results in an increase in Langmuir sorption in the fluorinated materials relative to the unfluorinated base polymer. The increase in diffusion coefficients was attributed to the increase in FFV, as corroborated by positron annihilation lifetime spectroscopy [167].

1.5.3 Polar and Hydrogen Bonding Side-chains

The degree of polarity and hydrogen bonding in side-chains or vinyl groups can cause a significant increase in interactions between polymer chains. This increased interchain interaction raises T_g and density in such polymers, as shown in Table 1.12 [168–170]. These effects can also contribute to significant levels of crystallinity in such materials, and crystallinity can strongly reduce gas permeability. The strength of the polarity or hydrogen bonding strongly influences the gas permeability; decreases in chain mobility are observed when polarity and hydrogen bonding increase. For example, polar polyacrylonitrile is over six orders of magnitude less permeable to CO_2 than 1,2-polybutadiene. Dry poly(vinyl alco-

Table 1.11 Effect of fluorinated side-chains on transport properties of polynorbornenes[a] [167]. Reprinted with permission from Y. P. Yampolskii *et al.*, *Macromolecules*, **27**, 2872–2878 (1994). Copyright (1994) American Chemical Society

Structure	T_g (°C)	FFV	P_{CO_2} (barrer)	α_{CO_2/CH_4}	$D_{CO_2} \times 10^7$ (cm^2/s)	$S_{CO_2} \times 10^2$ cm^3 (STP)/(cm^3 atm)
 Polynorbornene	31	0.156	15.4	6.3	1.6	0.96
 Poly(5,5-difluoro-6,6-bis (trifluoromethylnorbornene))	169	0.165	200	15.4	0.84	24
 Poly(5,5,6-trifluoro-6-neptafluoropropoxynorbornene)	77	0.187	200	11	4.0	5.0

[a]Permeability and diffusivity experiments were conducted at 22 °C, the feed pressure was held steady in a range from 0.01 to 0.65 atm, and the downstream pressure ranged from 0 to 0.01 atm; sorption experiments were conducted at 25 °C.

hol) is three orders of magnitude less permeable to CO_2 than polar poly(vinyl chloride), which shows that hydrogen bonding between polymer chains severely inhibits gas permeation.

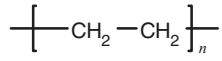
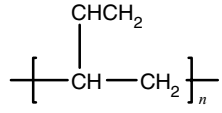
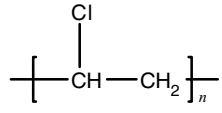
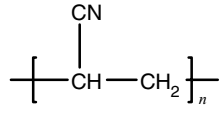
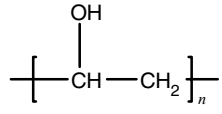
1.5.4 Para *versus* Meta *Linkages*

In polymers with aromatic backbones, such as polysulfones, changing the aromatic structure from *para* to *meta* reduces the T_g and FFV, as indicated in Table 1.13 [158,159]. *Meta*-connected materials pack more efficiently than analogous *para*-configured polymers [158]. Moreover, chain mobility is impeded in the *meta*-configuration since any significant motion of these segments require multisegment co-operation, whereas *para*-connected phenyl rings require much less co-operative motion for rotation. Both of these effects contribute to reducing the FFV of *meta*-connected polysulfones relative to that of their *para*-connected analogs. The *meta*-configuration has consistently lower permeability, solubility and diffusivity than the equivalent *para*-connected polymer due to lower FFV and T_g in the *meta*-connected material. The influence of *para*/*meta* connections on gas transport properties in polysulfones is consistent with similar data for other families of glassy polymers, such as polyesters and polyimides [76]. This effect has recently been the focus of molecular modeling studies which confirm these experimental observations [171].

1.5.5 Cis/Trans *Configuration*

The packing efficiency of polymers with unsaturated backbones depends on the amount of *cis* and *trans* configurations of the double bond. For poly(*tert*-butylacetylene), the packing efficiency increased as the *cis* content increased [172].

Table 1.12 Effect of vinyl polar groups on physical properties and gas transport. Reprinted from *Journal of Membrane Science*, **2**, S. M. Allen, M. Fujii, V. T. Stannett, H. B. Hopfenberg and J. L. Williams, 'The barrier properties of polyacrylonitrile', 153–163, Copyright (1977), with permission from Elsevier

Polymer	Structure	T_g (°C) [161]	Density (g/cm^3) [161]	P_{CO_2} (barrer)[a]
Polyethylene (PE)		−44	1.008	35.2 [162]
Poly(1,2-butadiene) (PB)		−50	0.950	138 [162]
Poly(vinyl chloride) (PVC)		81	1.450	0.029 [162]
Polyacrylonitrile (PAN)		125	1.125	0.000 28 [152]
Poly(vinyl alcohol) (PVOH)		85	1.291	0.000 02 [163]

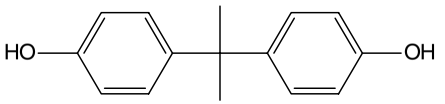
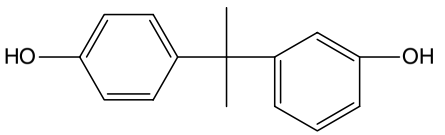
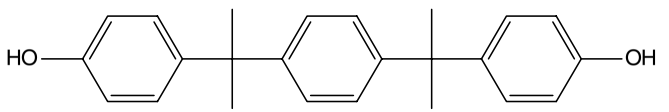
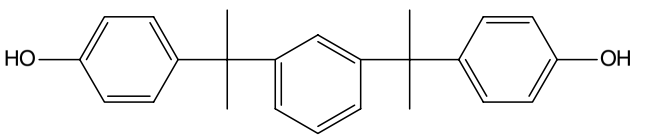
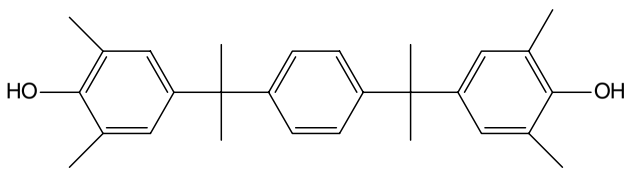
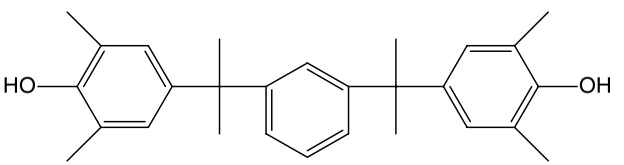
[a]Data reported at 30 °C for PE, PB and PVC, at 25 °C for PAN and at 23 °C for PVOH.

As the *cis* content increased, the gas diffusion coefficients increased initially and reached a maximum at a *cis* content of 50.2 %, as shown in Figure 1.21(a). At higher *cis* content, diffusivity decreased monotonically. Gas solubility also decreased at higher *cis* content in this polymer. The reduction in gas sorption was linked to a decrease in Langmuir sorption sites (cf. Figure 1.21(b)), which is consistent with a loss in excess free volume at higher *cis* contents (cf. Equation (1.38)). The reduction in diffusivity was also consistent with the increased chain packing efficiency at higher *cis* contents. It was speculated that chains with very high levels of *cis* or *trans* linkages formed rather regular helical structures that might pack very efficiently in the solid state, which would lead to reductions in FFV and, in turn, solubility and diffusivity. Polymers with intermediate concentrations of *cis* or *trans* linkages were thought to yield more disordered polymer structures, which packed less efficiently in the solid-state, which would lead to higher FFV, solubility and diffusivity. Similar gas transport behavior has been observed in other unsaturated polymers such as poly(trimethylsilyl norbornene) [173] and poly(methacrylate azobenzene) [174].

1.6 Conclusions

Gas and vapor transport is described by the 'solution–diffusion' concept, where permeability is the product of solubility and diffusivity. Both the solubility and diffusion coefficients are polymer- and penetrant-dependent. Although polymer structure and properties influence gas and vapor transport, there are very few parameters that apply universally. One of the few parameters that does correlate well with changes in gas transport in polymers is the fractional free volume (FFV). The latter is an indication of the open volume between polymer chains through which penetrant molecules can pass. Changes in polymer structure do not consistently affect gas transport behavior. However, altering polymer structure within closely related polymer families

Table 1.13 Effect of *meta/para* configuration in aroamtic polysulfones on transport properties[a] [159]. Reprinted with permission from C. L. Aitken *et al.*, *Macromolecules*, **25**, 3424–3434 (1992). Copyright (1992) American Chemical Society

Bisphenol monomer	T_g (°C)	FFV	ρ (g/cm^3)	P_{CO_2} (barrer)	α_{CO_2/CH_4}	$D_{CO_2} \times 10^8$ (cm^2/s)	S_{CO_2} cm^3 (STP)/(cm^3 atm)
 (PSF)	186	0.156	1.24	5.6	22	2.0	2.1
 (3,4'-PSF)	156	0.149	1.25	1.5	29	0.9	1.3
 (PSF-P)	191	0.156	1.191	6.8	20	3.2	2.1
 (PSF-M)	140	0.151	1.201	2.8	25	2.7	1.1
 (TMPSF-P)	214	0.168	1.127	13	22	5.0	2.0
 (TMPSF-M)	175	0.158	1.141	7.0	25	4.5	1.6

[a]Permeability and solubility measurements were conducted at 35 °C, 10 atm feed pressure and a permeate pressure 'at vacuum'.

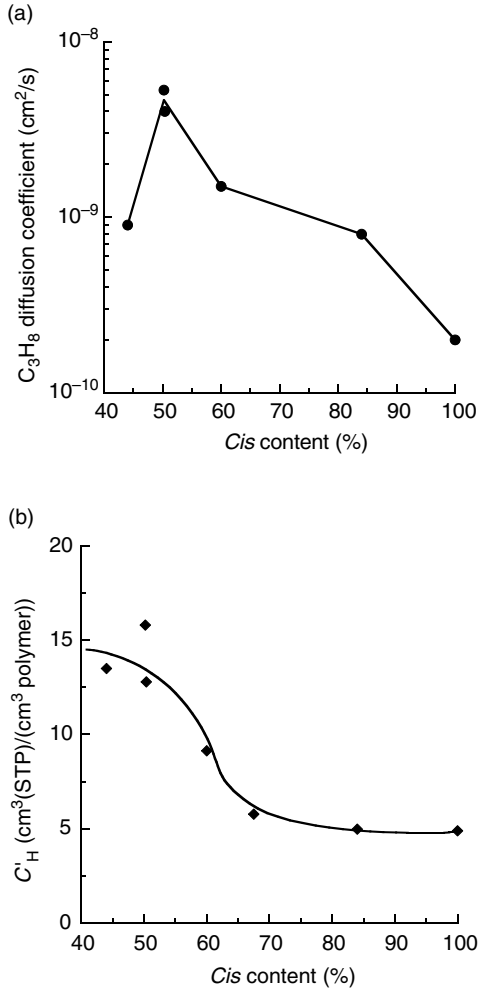


Figure 1.21 Relationship between *cis* isomer content in poly(*tert*-butylacetylene) and (a) infinite diffusion coefficient at 35 °C and (b) Langmuir capacities at 35 °C [172]. (a, b) From 'The influence of chain configuration and, in turn, chain packing on the sorption and transport properties of poly(*tert* butyl acetylene)', A. Morisato, N. R. Miranda, B. D. Freeman and H. B. Hopfenberg, *J. Appl. Polym. Sci.,* **49**, 2065–2074, Copyright © 1993, John Wiley & Sons, Inc. Reprinted with permission of John Wiley & Sons, Inc.

does have the ability to significantly influence solubility and diffusivity via changes in T_g and FFV. Structural changes which increase the efficiency of polymer chain packing cause FFV to decrease and also decrease the permeability. Diffusion coefficients decrease with increasing penetrant size. Solubility is related to the condensability of the penetrant and generally increases with increasing T_c of the penetrant.

Pressure and temperature strongly influence gas and vapor transport in polymers. Increasing the pressure increases the solubility according to Henry's law in rubbery polymers, and dual-mode sorption in glassy polymers. Increasing temperature generally has the opposite effect. Diffusivity for non-interacting, low-sorbing gases is largely independent of pressure; however, diffusivity for highly sorbing gases is strongly dependent on pressure (i.e. plasticization).

Finally, mixed-gas permeation properties do not necessarily correlate with those obtained in pure-gas measurements. In ideal, non-interactive cases, such as oxygen/nitrogen or hydrogen/methane separation, pure-gas permeability and selectivity are essentially identical to mixed-gas permeability and selectivity. However, separations involving condensable, highly sorbing feed components, such as carbon dioxide or organic vapors, can suffer from plasticization or competitive sorption, each of which often lowers selectivity. In addition, non-idealities, which can generally be neglected in pure-gas measurements, even at high pressure, require the use of fugacity for accurate analysis in mixed-gas systems. Other systems, such as reverse-selective vapor separations, actually exhibit better mixed-gas separation properties than pure-gas separation properties, and so plasticization and enhanced solubility selectivity effects can also act to improve separation performance in these cases.

References

[1] D. R. Paul, 'The solution-diffusion model for swollen membranes', *Separation and Purification Methods*, **5** (1976), 33–50.

[2] J. G. Wijmans and R. W. Baker, 'The solution-diffusion model: a review', *Journal of Membrane Science*, **107** (1995), 1–21.

[3] J. K. Mitchell, 'On the penetrativeness of fluids', *Journal of Membrane Science*, **100** (1995), 11–16.

[4] T. Graham, 'On the absorption and dialytic separation of gases by colloid septa. Action of a septum of caoutchouc', *Philosophical Magazine*, **32** (1866), 401–420.

[5] S. von Wroblewski, 'Ueber die natur der absorption der gase durch flussigkeiten unter hohen drucken', *Ann Physik u Chem*, **8** (1879), 29–52.

[6] K. W. Boeddeker, 'Commentary Tracing Membrane Science', *Journal of Membrane Science*, Special Issue: The Early History of Membrane Science, **100** (1995), 1–68.

[7] K. Ghosal and B. D. Freeman, 'Gas separation using polymer membranes: An overview', *Polymers for Advanced Technology*, **5** (1994), 673–697.

[8] J. H. Petropoulos, 'Mechanisms and theories for sorption and diffusion of gases in polymers', in D. R. Paul and Y. P. Yampolskii (Eds), *Polymeric Gas Separation Membranes*, CRC Press, Boca Raton, FL, USA (1994), pp. 17–82.

[9] R. M. Felder and G. S. Huvard, *Permeation, Diffusion and Sorption of Gases and Vapors*, Methods of Experimental Physics, Vol. 16C, Academic Press, New York, NY, USA (1980), pp. 315–377.

[10] H. Lin and B. D. Freeman, *Permeation and Diffusion*, Springer-Handbook of Materials Measurement Methods, Vol. 16C, Springer-Verlag, Berlin, Germany (2005).

[11] W. J. Koros and C. M. Zimmerman, 'Transport and Barrier Properties', in R. F. J. Brady (Ed.), *Comprehensive Desk Reference of Polymer Characterization and Analysis*, Oxford University Press, Washington, DC, USA (2003), pp. 680–699.

[12] V. Bondar, B. D. Freeman and Y. P. Yampolskii, 'Sorption of gases and vapors in an amorphous glassy perfluorodioxide copolymer', *Macromolecules*, **32** (1999), 6163–6171.

[13] V. I. Bondar, B. D. Freeman and I. Pinnau, 'Gas sorption and characterization of poly(ether-*b*-amide) segmented block copolymers', *Journal of Polymer Science, Part B: Polymer Physics,* **37** (1999), 2463–2475.

[14] S. N. Dhoot, B. D. Freeman and M. Stewart, 'Sorption and transport of linear esters and branched alkanes in biaxially oriented poly (ethylene terephthalate)', *Industrial and Engineering Chemistry Research*, **43** (2004), 2966–2976.

[15] V. T. Stannett, W. J. Koros, D. R. Paul and H. K. Lonsdale, 'Recent advances in membrane science and technology', *Advances in Polymer Science*, **32** (1979), 69–121.

[16] I. Pinnau and B. D. Freeman, *Membrane Formation and Modification Overview*, in I. Pinnau and B. D. Freeman (Eds.) American Chemical Society Symposium Series 744, American Chemical Society, Washington, D.C, (2000), pp. 1–22.

[17] W. J. Koros and I. Pinnau, 'Membrane formation for gas separation processes', in D. R. Paul and Y. P. Yampolskii (Eds), *Polymeric Gas Separation Membranes*, CRC Press, Boca Raton, FL, USA (1994), pp. 209–272.

[18] L. M. Robeson, 'Correlation of separation factor versus permeability for polymeric membranes', *Journal of Membrane Science*, **62** (1991), 165–185.

[19] D. T. Coker, B. D. Freeman and G. K. Fleming, 'Modeling multicomponent gas separation using hollow-fiber membrane contactors', *AIChE Journal*, **44** (1998), 1289–1302.

[20] A. Y. Alentiev and Y. P. Yampolskii, 'Free volume model and tradeoff relations of gas permeability and selectivity in glassy polymers', *Journal of Membrane Science*, **165** (2000), 201–216.

[21] B. D. Freeman, 'Basis of permeability/selectivity tradeoff relations in polymeric gas separation membranes', *Macromolecules*, **32** (1999), 375–380.

[22] D. W. Breck, *Zeolite Molecular Sieves: Structure, Chemistry and Use*, John Wiley & Sons, Inc. New York, NY, USA (1974), pp. 593–724.

[23] S. A. Stern, 'Polymers for gas separations: The next decade', *Journal of Membrane Science*, **94** (1994), 1–65.

[24] M. Cohen and T. Turnbull, 'Molecular transport in liquids and glasses', *Journal of Chemical Physics*, **31** (1959), 1164–1169.

[25] R. W. Baker, 'Future directions of membrane gas separation technology', *Industrial and Engineering Chemistry Research*, **41** (2002), 1393–1411.

[26] R. W. Baker, J. G. Wijmans and J. H. Kaschemekat, 'The design of membrane vapor–gas separation systems', *Journal of Membrane Science*, **151** (1998), 55–62.

[27] X. Wang, R. Daniels and R. W. Baker, 'Recovery of VOCs from high-volume, low-VOC-concentration air systems', *AIChE Journal*, **47** (2001), 1094–1100.

[28] B. D. Freeman and I. Pinnau, 'Separation of gases using solubility-selective polymers', *Trends in Polymer Science*, **5** (1997), 167–173.

[29] D. V. Laciak, L. M. Robeson and C. D. Smith, 'Group contribution modeling of gas transport in polymeric membranes', in B. D. Freeman and I. Pinnau (Eds), *Polymer Membranes for Gas and Vapor Separations*, ACS Symposium Series 733, American Chemical Society, Washington, DC, USA (1999), pp. 151–177.

[30] J. Y. Park and D. R. Paul, 'Correlation and prediction of gas permeability in glassy polymer membrane materials via modified free volume based group contribution method', Journal of Membrane Science, **125** (1997), 23–39.

[31] D. W. van Krevelen, *Properties of Polymers*, 3rd Edn., Elsevier, Amsterdam, The Netherlands (1990).

[32] H. Lin and B. D. Freeman, 'Gas solubility, diffusivity and permeability in poly(ethylene oxide)', *Journal of Membrane Science*, **239** (2004), 105–117.

[33] A. S. Michaels and H. J. Bixler, 'Flow of gases through polyethylene', *Journal of Polymer Science*, **50** (1961), 412–439.

[34] T. C. Merkel, V. Bondar, K. Nagai, B. D. Freeman and I. Pinnau, 'Gas sorption, diffusion, and permeation in poly(dimethylsiloxane)', *Journal of Polymer Science, Part B: Polymer Physics*, **38** (2000), 415–434.

[35] A. S. Michaels, W. R. Vieth and J. A. Barrie, 'Diffusion of gases in polyethylene terephthalate', *Journal of Applied Physics*, **34** (1963), 13–21.

[36] G. J. van Amerongen, 'Diffusion in Elastomers', *Rubber Chemistry and Technology*, **37** (1964), 1065–1153.

[37] V. V. Teplyakov and S. G. Durgaryan, 'Correlation analysis of permeation parameters for polymers', *Vysokomolekuliarnye Soedineniia (Polymer Science, Series A)*, **26** (1984), 1498–1505.

[38] V. V. Teplyakov and P. Meares, 'Correlation aspects of the selective gas permeabilities of polymeric materials and membranes', *Gas Separation and Purification*, **4** (1990), 66–73.

[39] V. P. Shantarovich, I. B. Kevdina, Y. P. Yampolskii and A. Y. Alentiev, 'Positron annihilation lifetimes of high and low free volume glassy polymers: effects of free volume sizes on the permeability and permselectivity', *Macromolecules*, **33** (2000), 7453–7466.

[40] P. Meares, 'The diffusion of gases through polyvinyl acetate', *Journal of the American Chemical Society*, **76** (1954), 3415–3422.

[41] G. S. Park, *Transport Principles-Solution, Diffusion and Permeation in Polymer Membranes*, NATO ASI Series, Series C, 181 Kluwer Academic Publishers, Dordrecht, The Netherlands (1986), pp. 57–107.

[42] P. E. J. Rouse, 'Diffusion of vapors in films', *Journal of the American Chemical Society*, **69** (1947), 1068–1073.

[43] J. D. Wellons and V. T. Stannett, 'Permeation, sorption, and diffusion of water in ethyl cellulose', *Journal of Polymer Science*, **4** (1966), 593–602.

[44] K. A. Schult and D. R. Paul, 'Water sorption and transport in a series of polysulfones', *Journal of Polymer Science, Part B: Polymer Physics*, **34** (1996), 2805–2817.

[45] K. Ghosal, R. T. Chern and B. D. Freeman, 'Effect of basic substituents on gas sorption and permeation in polysulfone', *Macromolecules*, **29** (1996), 4360–4369.

[46] E. L. Spotz, The equation of state of gases at low and moderate densities, in J. O. Hirschfelder, C. F. Curtiss and R. B. Bird (Eds), *Molecular Theory of Gases and Liquids*, Structure of Matter Series, John Wiley & Sons, Inc., New York, USA (1954), pp. 131–230.

[47] T. Titani, 'Viscosity of vapors of organic compounds. II', *Bulletin of the Chemical Society of Japan*, **5** (1930), 98–108.

[48] B. E. Poling, J. M. Prausnitz and J. P. O'Connell, *The Properties of Gases and Liquids*, 5th Edn, McGraw-Hill, New York, NY, USA (2000).

[49] T. H. Chung, M. Ajlan, L. L. Lee and K. E. Starling, 'Generalized multiparameter correlation for nonpolar and polar fluid transport properties', *Industrial and Engineering Chemistry Research*, **27** (1988), 671–679.

[50] T. H. Chung, L. L. Lee and K. E. Starling, 'Application of kinetic gas theories and multiparameter correlation for prediction of dilute gas viscosity and thermal conductivity', *Industrial and Engineering Chemistry Research*, **23** (1984), 8–13.

[51] E. L. Spotz, 'Transport phenomena of dilute gases', in J. O. Hirschfelder, C. F. Curtiss and R. B. Bird (Eds), *Molecular Theory of Gases and Liquids*, Structure of Matter Series, John Wiley & Sons, Inc., New York, NY, USA (1954), pp. 131–230.

[52] J. S. Rowlinson, 'The second virial coefficients of polar gases', *Transactions of the Faraday Society*, **45** (1949), 974–984.

[53] L. S. Tee, S. Gotoh and W. E. Stewart, 'Molecular parameters for normal fluids. The Lennard-Jones 12-6 potential', *Industrial and Engineering Chemistry Research*, **5** (1966), 346–363.

[54] W. M. Lee, 'Selection of barrier materials from molecular structure', *Polymer Engineering and Science*, **20** (1980), 65–69.

[55] A. Reynier, P. Dole, S. Humbel and A. Feigenbaum, 'Diffusion coefficients of additives in polymers. I. Correlation with geometric parameters', *Journal of Applied Polymer Science*, **82** (2001), 2422–2433.

[56] H. Fujita, A. Kishimoto and K. Matsumo, 'Concentration and temperature dependence of diffusion coefficients', *Transactions of the Faraday Society*, **56** (1960), 424–437.

[57] Y. P. Yampolskii, S. G. Durgaryan and N. S. Nametkin, 'Permeability, diffusivity, and solubility of *n*-alkenes in polymers', *Vysokomolekuliarnye Soedineniia (Polymer Science, Series B)*, **21** (1979), 616–621.

[58] S. N. Dhoot, B. D. Freeman, M. Stewart and A. J. Hill, 'Sorption and transport of linear alkane hydrocarbons in biaxially oriented poly(ethylene terephthalate)', *Journal of Polymer Science, Part B: Polymer Physics*, **39** (2001), 1160–1172.

[59] K. Tanaka, A. Taguchi, J. Hao, H. Kita and K. Okamoto, 'Permeation and separation properties of polyimide membranes to olefins and paraffins', *Journal of Membrane Science*, **121** (1996), 197–207.

[60] B. D. Freeman and I. Pinnau, 'Polymeric materials for gas separations', in B. D. Freeman and I. Pinnau (Eds), *Polymer Membranes for Gas and Vapor Separations*, ACS Symposium Series 733, American Chemical Society, Washington, DC, USA (1999), pp. 1–27.

[61] R. M. Barrer and G. Skirrow, 'Transport and equilibrium phenomena in gas elastomer systems. Part II. Equilibrium phenomena', *Journal of Polymer Science*, **3** (1948), 564–575.

[62] T. C. Merkel, V. Bondar, K. Nagai and B. D. Freeman, 'Sorption and transport of hydrocarbon and perfluorocarbon gases in poly(1-trimethylsilyl-1-propyne)', *Journal of Polymer Science, Part B: Polymer Physics*, **38** (1999), 273–296.

[63] G. Gee, 'Some thermodynamic properties of high polymers and their molecular interpretation, *Quarterly Reviews of the Chemical Society*, **1** (1947), 265–298.

[64] Y. P. Yampolskii and V. V. Volkov, 'Studies in gas permeability and membrane gas separation in the Soviet Union', *Journal of Membrane Science*, **64** (1991), 191–228.

[65] W. J. Koros, D. R. Paul and G. S. Huvard, 'Energetics of gas sorption in glassy polymers', *Polymer*, **20** (1979), 956–960.

[66] F. Korosy, 'Two rules concerning solubility of gases and crude data on solubility of krypton', *Transactions of the Faraday Society*, **33** (1937), 416–425.

[67] R. Prabhakar, M. G. De Angelis, G. C. Sarti, B. D. Freeman and M. C. Coughlin, 'Gas and vapor sorption, permeation and diffusion in poly(tetrafluoroethylene-*co*-perfluoromethyl vinyl ether)' Macromolecules, **38** (2005), 1899–1910.

[68] Y. Kamiya, Y. Naito, K. Terada and K. Mizoguchi, 'Volumetric properties and interaction parameters of dissolved gases in poly(dimethylsiloxane) and polyethylene', *Macromolecules*, **33** (2000), 3111–3119.

[69] K. Toi, G. Morel and D. R. Paul, 'Gas sorption and transport in poly(phenylene oxide) and comparisons with other glassy polymers', *Journal of Applied Polymer Science*, **27** (1982), 2997–3005.

[70] A. S. Michaels and H. J. Bixler, 'Solubility of gases in polyethylene', *Journal of Polymer Science*, **50** (1961), 393–412.

[71] G. E. Serad, B. D. Freeman, M. E. Stewart and A. J. Hill, 'Gas and vapor sorption and diffusion in poly(ethylene terephthalate)', *Polymer*, **42** (2001), 6929–6943.

[72] K. Ghosal, R. T. Chern, B. D. Freeman and R. Savariar, 'The effect of aryl nitration on gas sorption and permeation in polysulfone', *Journal of Polymer Science, Part B: Polymer Physics*, **33** (1995), 657–666.

[73] D. R. Stull, E. F. Westrum and G. C. Sinke, *The Chemical Thermodynamics of Organic Compounds*, John Wiley & Sons, Inc., New York, NY, USA (1969).

[74] S. A. Stern, J. T. Mullhaupt and P. J. Garries, 'The effect of pressure on the permeation of gases and vapors through polyethylene. Usefulness of the corresponding states principle', *AIChE Journal*, Special Issue: The Early History of Membrane Science, **15** (1969), 64–73.

[75] Y. P. Yampolskii, D. Wiley and C. Maher, 'Novel correlation for solubility of gases in polymers: effect of molecular surface area of gases', *Journal of Applied Polymer Science*, **76** (2000), 552–560.

[76] M. R. Pixton and D. R. Paul, 'Relationships between structure and transport properties for polymers with aromatic backbones', in D. R. Paul and Y. P. Yampolskii (Eds), *Polymeric Gas Separation Membranes*, CRC Press, Boca Raton, FL, USA (1994), pp. 83–154.

[77] T. C. Merkel, B. D. Freeman, R. J. Spontak, Z. He, I. Pinnau, P. Meakin and A. J. Hill, Ultrapermeable, reverse-selective nanocomposite membranes', *Science*, **296** (2002), 519–522.

[78] I. Pinnau, C. G. Casillas, A. Morisato and B. D. Freeman, 'Hydrocarbon/hydrogen mixed gas permeation in poly(1-trimethylsilyl-1-propyne) (PTMSP), poly(1-phenyl-1-propyne) (PPP) and PTMSP/PPP blends', *Journal of Polymer Science, Part B: Polymer Physics*, **34** (1996), 2613–2621.

[79] Y. P. Yampolskii, S. G. Durgaryan and N. S. Nametkin, 'Translational and rotational mobility of low molecular mass compounds in polymers with different glass transition temperatures', *Vysokomolekuliarnye Soedineniia*, **24** (1982), 536–541.

[80] M. W. Fitch, W. J. Koros, R. L. Nolen and J. R. Carnes, 'Permeation of several gases through elastomers, with emphasis on the D_2/H_2 pair', *Journal of Applied Polymer Science*, **47** (1993), 1033–1046.

[81] Y. Kawakami, H. Karasawa, T. Aoki, Y. Yamamaura, H. Hisada and Y. Yamashita, 'Polymers with oligoorganosilicone side chains as materials for oxygen permeable membranes', *Polymer Journal*, **17** (1985), 1159–1172.

[82] Y. Kawakami, H. Toda, M. Higashino and Y. Yamashita, 'Polynorbornenes with oligodimethylsiloxanyl substituents for selectively oxygen permeable membrane material', *Polymer Journal*, **20** (1988), 285–292.

[83] Y. Hirayama, T. Yoshinaga, Y. Kusuki, K. Ninomiya, T. Sakakibara and T. Tamari, 'Relation of gas permeability with structure of aromatic

polyimides I', *Journal of Membrane Science*, **111** (1996), 169–182.

[84] K. Nagai, T. Masuda, T. Nakagawa, B. D. Freeman and I. Pinnau, 'Poly[1-(trimethylsilyl)-1-propyne] and related polymers: synthesis, properties and functions', *Progress in Polymer Science*, **26** (2001), 721–798.

[85] R. T. Chern, W. J. Koros, E. S. Sanders and R. Yui, 'Second Component effects in sorption and permeation of gases in glassy polymers', *Journal of Membrane Science*, **15** (1983), 157–169.

[86] A. R. Berens and H. B. Hopfenberg, 'Diffusion of organic vapors at low concentrations in glassy PVC, polystyrene and PMMA', *Journal of Membrane Science*, **10** (1982), 283–303.

[87] R. T. Chern, W. J. Koros, H. B. Hopfenberg and V. T. Stannett, 'Material selection for membrane-based gas separations', in D. R. Lloyd (Ed.), Material Science of Synthetic Membranes, ACS Symposium Series 269, American Chemical Society, Washington, DC, USA (1985), pp. 25–46.

[88] T. C. Merkel, V. Bondar, K. Nagai, B. D. Freeman and Y. P. Yampolskii, 'Gas sorption, diffusion and permeation in poly(2,2-bis(trifluoromethyl)-4,5-difluoro-1,3-dioxole-co-tetrafluoroethylene)', *Macromolecules*, **32** (1999), 8427–8440.

[89] K. Toi and D. R. Paul, 'Effect of polystyrene molecular weight on the carbon dioxide sorption isotherm', *Macromolecules*, **15** (1982), 1104–1107.

[90] H. Lin, B. D. Freeman, L. G. Toy, V. Bondar, R. P. Gupta, S. J. Pas and A. J. Hill, 'Reverse-selective polymeric membranes for hydrogen purification', *Polymer Preprints (American Chemical Society Division of Polymer Chemistry)*, **45** (1) (2004), 23–24.

[91] L. A. Pilato, L. M. Litz, B. Haritay, A. G. Farnham, J. H. Kawakami, P. E. Fritze and J. E. McGrath, 'Polymers for permselective membrane gas separations', *Polymer Preprints (American Chemical Society Division of Polymer Chemistry)*, **161** (1) (1975), 41–46.

[92] S. G. Charati, A. Y. Houde and S. S. Kulkarni, 'Transport of gases in aromatic polyesters: correlation with WAXD studies', *Journal of Polymer Science, Part B: Polymer Physics*, **29** (1991), 921–931.

[93] A. Bondi, *Physical Properties of Molecular Crystals, Liquids and Gases*, John Wiley & Sons, Inc., New York, NY, USA (1968).

[94] J. S. Vrentas and C. M. Vrentas, 'Predictive methods for self-diffusion and mutual diffusion coefficients in polymer–solvent systems', *European Polymer Journal*, **34** (1998), 797–803.

[95] J. L. Duda, Y. C. Ni and J. S. Vrentas, 'An equation relating self-diffusion and mutual diffusion coefficients in polymer-solvent systems', *Macromolecules*, **12** (1979), 459–462.

[96] A. Puleo, N. Muruganandam and D. R. Paul, 'Gas sorption and transport in substituted polystyrenes', *Journal of Polymer Science, Part B: Polymer Physics*, **27** (1989), 2385–2406.

[97] D. H. Weinkauf and D. R. Paul, 'Gas transport properties of thermotropic liquid-crystalline copolyestyers. II. The effects of copolymer composition', *Journal of Polymer Science, Part B: Polymer Physics*, **30** (1992), 837–849.

[98] R. R. Light and R. W. Seymour, 'Effect of sub-T_g relaxations on the gas transport properties of polyesters', *Polymer Engineering and Science*, **22** (1982), 857–864.

[99] D. H. Weinkauf and D. R. Paul, 'Gas transport properties of thermotropic liquid-crystalline copolyesters. I. The effects of orientation and annealing', *Journal of Polymer Science, Part B: Polymer Physics*, **30** (1992), 813–835.

[100] D. H. Weinkauf and D. R. Paul, 'Gas transport properties of liquid crystalline poly(ethylene terephthalate-*co-p*-oxybenzoate)', *Journal of Polymer Science, Part B: Polymer Physics*, **29** (1991), 329–340.

[101] H. Lin and B. D. Freeman, 'Gas permeation and diffusion in crosslinked poly(ethylene glycol diacrylate)', *Macromolecules*, **38** (2005), 8394–8407.

[102] J. S. McHattie, W. J. Koros and D. R. Paul, 'Gas transport properties in polysulfones. 3. Comparison of tetramethyl-substituted bisphenols', *Polymer*, **33** (1992), 1701–1711.

[103] A. Thran, G. Kroll and F. Faupel, 'Correlation between fractional free volume and diffusivity of gas molecules in glassy polymers', *Journal of Polymer Science, Part B: Polymer Physics*, **37** (1999), 3344–3358.

[104] C. Nagel, K. Guenther-Schade, D. Frisch, T. Strunskus and F. Faupel, 'Free volume and transport properties in highly selective polymer membranes', *Macromolecules*, **35** (2002), 2071–2077.

[105] A. Y. Alentiev and Y. P. Yampolskii, 'Meares equation and the role of cohesion energy density in diffusion in polymers', *Journal of Membrane Science*, **206** (2002), 291–306.

[106] A. Singh, B. D. Freeman and I. Pinnau, 'Pure and mixed gas acetone/nitrogen permeation properties of polydimethylsiloxane', *Journal of Polymer Science, Part B: Polymer Physics*, **32** (1998), 289–301.

[107] P. J. Flory and J. J. Rehner, 'Statistical mechanics of cross-linked polymer networks II. Swelling', *The Journal of Chemical Physics*, **11** (1943), 521–526.

[108] G. K. Fleming and W. J. Koros, 'Dilation of polymers by sorption of carbon dioxide at elevated pressures. 1. Silicone rubber and

unconditioned polycarbonate', *Macromolecules*, **19** (1986), 2285–2291.

[109] Y. Yang, Y. Huang, D. Wang, H. Liu and C. Hu, 'Sorption and diffusion of ethanol vapor in polybutadiene/acrylonitrile, polybutadiene/styrene and polybutadiene based polyurethanes', *European Polymer Journal*, **40** (2004), 855–863.

[110] J. A. Barrie, 'Water in polymers', in J. Crank and G. S. Park (Eds), *Diffusion in Polymers*, Academic Press, New York, NY, USA (1968), pp. 259–314.

[111] M. G. De Angelis, T. C. Merkel, V. Bondar, B. D. Freeman, F. Doghieri and G. C. Sarti, 'Hydrocarbon and fluorocarbon solubility and dilation in poly(dimethylsiloxane): Comparison of experimental data with predictions of the Sanchez–Lacombe equation of state', *Journal of Polymer Science, Part B: Polymer Physics*, **37** (1999), 3011–3026.

[112] D. R. Paul, 'Gas sorption and transport in glassy polymers', *Berichte der Bunsen-Gesellschaft*, **83** (1979), 294–302.

[113] R. Patterson and Y. P. Yampolskii, 'Solubility of gases in glassy polymers', *Journal of Physical Chemistry Reference Data*, **28** (1999), 1255–1450.

[114] A. Tokarev, K. Friess, J. Machkova, M. Sipek and Y. P. Yampolskii, 'Sorption and diffusion of organic vapors in amorphous Teflon AF2400', *Journal of Polymer Science, Part B: Polymer Physics*, (2000), Vol. 44(5), (2006) 832–844.

[115] W. J. Koros and R. T. Chern, 'Separation of gaseous mixtures using polymer membranes', in R. W. Rousseau (Ed.), *Handbook of Separation Progress Technology*, John Wiley & Sons, Inc., New York, NY, USA (1987), pp. 862–953.

[116] W. J. Koros and D. R. Paul, 'Carbon dioxide sorption in poly(ethylene terephthalate) above and below the glass transition', *Journal of Polymer Science, Part B: Polymer Physics*, **16** (1978), 1947–1963.

[117] V. V. Volkov, A. K. Bokarev, S. G. Durgaryan and N. S. Nametkin, 'Sorption of low-molecular-weight compounds in glassy PVTMS in vicinity and below the critical temperature of the solute', *Doklady Akademie Nauk SSSR*, **282** (1985), 641–644.

[118] S. M. Jordan and W. J. Koros, 'Characterization of CO_2-induced conditioning of substituted polycarbonates using various "exchange" penetrants', *Journal of Membrane Science*, **51** (1990), 233–247.

[119] S. M. Jordan, M. A. Henson and W. J. Koros, 'The effects of carbon dioxide conditioning on the permeation behavior of hollow fiber asymmetric membranes', *Journal of Membrane Science*, **54** (1990), 103–118.

[120] V. Bondar, Y. Kamiya and Y. P. Yampolskii, 'On pressure dependence of the parameters of the dual-mode sorption model', *Journal of Polymer Science, Part B: Polymer Physics*, **34** (1996), 369–378.

[121] A. R. Berens, 'The solubility of vinyl chloride in poly(vinyl chloride)', *Die Angewandte Makromolekulare Chemie*, **47** (1975), 97–110.

[122] A. Y. Alentiev, V. P. Shantarovich, T. C. Merkel, V. Bondar, B. D. Freeman and Y. P. Yampolskii, 'Gas and vapor sorption, permeation, and diffusion in glassy amorphous Teflon AF1600', *Macromolecules*, **35** (2002), 9513–9522.

[123] C. Staudt-Bickel and W. J. Koros, 'Improvement of CO_2/CH_4 separation characteristics of polyimides by chemical crosslinking', *Journal of Membrane Science*, **155** (1999), 145–154.

[124] R. T. Chern and C. N. Provan, 'Gas-induced plasticization and the permselectivity of poly(tetrabromophenolphthalein) to a mixture of carbon dioxide and methane', *Macromolecules*, **24** (1991), 2203–2207.

[125] S. Zhou and S. A. Stern, 'The effect of plasticization on the transport of gases in and through glassy polymers', *Journal of Polymer Science, Part B: Polymer Physics*, **27** (2003), 205–222.

[126] H. Lin and B. D. Freeman, 'Gas and vapor solubility in crosslinked poly(ethylene glycol diacrylate)', *Macromolecules*, **38** (2005), 8394–8407.

[127] A. A. Armstrong and V. T. Stannett, 'Temperature effects during the sorption and desorption of water vapor in high polymers. I. Fibers, with particular reference to wool', *Makromolekulare Chemie*, **90** (1966), 145–160.

[128] W. J. Koros, D. R. Paul and A. A. Rocha, 'Carbon dioxide sorption and transport in polycarbonate', *Journal of Polymer Science, Part B: Polymer Physics*, **14** (1976), 687–702.

[129] V. T. Stannett, 'The transport of gases in synthetic polymer membranes – a historic perspective', *Journal of Membrane Science*, **3** (1978), 97–115.

[130] H. Lin, E. van Wagner, B. D. Freeman and I. Roman, 'High performance polymer membranes for natural gas sweetening', Advanced Materials, **18** (2006), 39–44.

[131] T. S. Chow, 'Molecular interpretation of glass transition temperature of polymer-diluent systems', *Macromolecules*, **13** (1980), 362–364.

[132] I. Pinnau and Z. He, 'Pure- and mixed-gas permeation properties of polydimethylsiloxane for hydrocarbon/methane and hydrocarbon/hydrogen

separation', *Journal of Membrane Science*, **244** (2004), 227–233.

[133] I. Pinnau and L. G. Toy, 'Transport of organic vapors through poly(1-trimethylsilyl-1-propyne)', *Journal of Membrane Science*, **116** (1996), 199–209.

[134] R. Ash, R. M. Barrer and P. Sharma, 'Sorption and flow of carbon dioxide and some hydrocarbons in a microporous carbon membrane', *Journal of Membrane Science*, **1** (1976), 17–32.

[135] R. Srinivasan, S. R. Auvil and P. M. Burban, 'Elucidating the mechanism(s) of gas transport in poly[1-(trimethylsilyl)-1-propyne] (PTMSP) membranes', *Journal of Membrane Science*, **86** (1994), 67–86.

[136] S. Y. Lee, B. S. Minhas and M. D. Donohue, 'Effect of gas composition and pressure on permeation through cellulose acetate membranes', *AIChE Symposium Series*, **84** (1988), 93–101.

[137] L. S. White, T. A. Blinka, H. A. Kloczewski and I.-F. Wang, 'Properties of a polyimide gas separation membrane in natural gas streams', *Journal of Membrane Science*, **103** (1995), 73–82.

[138] H. Lin, E. van Wagner, B. D. Freeman, L. G. Toy and P. Ragubuir, 'New membrane materials for CO_2/H_2 separation and a model for pure and mixed gas permeability', Science, **311** (2006), 639–642.

[139] A. Y. Houde, B. Krishnakumar, S. G. Charati and S. A. Stern, 'Permeability of dense (homogeneous) cellulose acetate membranes to methane, carbon dioxide, and their mixtures at elevated pressures', *Journal of Applied Polymer Science*, **62** (1996), 2181–2192.

[140] S. V. Dixon-Garrett, K. Nagai and B. D. Freeman, 'Ethylbenzene solubility, diffusivity and permeability in poly(dimethylsiloxane)', *Journal of Polymer Science, Part B: Polymer Physics*, **38** (2000), 1461–1473.

[141] H. Yasuda and T. Hirotsu, 'The effect of glass transition on gas permeability', *Journal of Applied Polymer Science*, **21** (1977), 105–112.

[142] R. M. Barrer, 'Permeability in relation to viscosity and structure of rubber', *Transactions of the Faraday Society*, **38** (1942), 322–331.

[143] G. J. van Amerongen, 'The permeability of different rubbers to gases and its relation to diffusivity and solubility', *Journal of Applied Physics*, **17** (1946), 972–985.

[144] R. Prabhakar, B. D. Freeman and I. Roman, 'Gas and vapor sorption and permeation in poly(2, 2, 4-trifluoro -5-trifluoromethoxy -1, 3-dioxle-co-tetrafluoroethylene)', *Macromolecules*, **37** (2004), 7688–7697.

[145] R. Prabhakar, R. Raharjo, L. G. Toy, H. Lin and B. D. Freeman, 'Self-consistent model of concentration and temperature dependence of permeability in rubbery polymers', *Industrial and Engineering Chemistry Research*, **44** (2005), 1547–1556.

[146] Y. P. Yampolskii, S. Shishatskii, A. Y. Alentiev and K. Loza, 'Correlations with and predictions of activation energies of gas permeation and diffusion in glassy polymers', *Journal of Membrane Science*, **148** (1998), 59–69.

[147] S. Glasstone, K. J. Laidler and H. Eyring, *The Theory of Rate Processes*, McGraw-Hill, New York, NY, USA (1941).

[148] S. A. Stern, V. M. Shah and B. J. Hardy, 'Structure-permeability relationship in silicone polymers', *Journal of Polymer Science, Part B: Polymer Physics*, **25** (1987), 1263–1298.

[149] W. J. Koros and G. K. Fleming, 'Membrane-based gas separation', *Journal of Membrane Science*, **83** (1993), 1–80.

[150] Y. P. Yampolskii and N. A. Plate, 'Is it possible to predict transport properties of polymers proceeding from chemical structure of the chains?', *Polymer Science*, **36** (1994), 1599–1609.

[151] H. Ohya, V. V. Kudryavtsev and S. I. Semenova, *Polyimide Membranes – Applications, Fabrications and Properties*, Gordon & Breach, Tokyo, Japan (1996).

[152] S. M. Allen, M. Fujii, V. T. Stannett, H. B. Hopfenberg and J. L. Williams, 'The barrier properties of polyacrylonitrile', *Journal of Membrane Science*, **2** (1977), 153–163.

[153] N. A. Plate and Y. P. Yampolskii, 'Relationship between structure and transport properties for high free volume polymeric materials', in D. R. Paul and Y. P. Yampolskii (Eds), *Polymeric Gas Separation Membranes*, CRC Press, Boca Raton, FL, USA (1994), pp. 155–207.

[154] V. S. Khotimskii, V. G. Filippova, I. S. Bryantseva, V. I. Bondar, V. P. Shantarovich and Y. P. Yampolskii, 'Synthesis, transport and sorption properties and free volume of polystyrene derivatives containing Si and F', *Journal of Applied Polymer Science*, **78** (2000), 1612–1620.

[155] E. S. Finkel'shtein, M. L. Gringolts, N. V. Ushakov, V. G. Lakhtin, S. A. Soloviev and Y. P. Yampolskii, 'Synthesis and gas permeation properties of new ROMP polymers from silyl substituted norbornadienes and norbornenes', *Polymer*, **44** (2003), 2843–2851.

[156] E. S. Finkel'shtein, K. L. Makovetskii, Y. P. Yampolskii, E. Portnykh, I. Ostrovskaya and N. Kaliuzhnyi, 'Ring-opening polymerization of norbornenes with organosilicon substituents. Gas permeability of polymers obtained', *Makromolekulare Chemie*, **192** (1991), 1–9.

[157] N. Muruganandam, W. J. Koros and D. R. Paul, 'Gas sorption and transport in substituted polycarbonates', *Journal of Polymer Science, Part B: Polymer Physics*, **25** (1987), 1999–2026.

[158] C. L. Aitken, W. J. Koros and D. R. Paul, 'Gas transport properties of bisphenol polysulfones', *Macromolecules*, **25** (1992), 3651–3658.

[159] C. L. Aitken, W. J. Koros and D. R. Paul, 'Effect of structural symmetry on gas transport properties of polysulfones', *Macromolecules*, **25** (1992), 3424–3434.

[160] W. J. Koros and G. K. Fleming, 'Membrane-based gas separation', *Journal of Membrane Science*, **83** (1993), 1–80.

[161] J. S. McHattie, W. J. Koros, D. R. Paul, 'Gas transport properties of polysulfones. 1. Role of symmetry of methyl group placement on bisphenol', *Polymer*, **32** (1991), 840–850.

[162] M. R. Pixton and D. R. Paul, 'Gas transport of polyarylates part II: Tetrabromination of the bisphenol', *Journal of Polymer Science, Part B: Polymer Physics*, **33** (1995), 1353–1364.

[163] M. Aguilar-Vega and D. R. Paul, 'Gas transport properties of polycarbonates and polysulfones with aromatic substitutions on the bisphenol connector group', *Journal of Polymer Science, Part B: Polymer Physics*, **31** (1993), 1599–1610.

[164] K. Ghosal, R. T. Chern, B. D. Freeman, W. H. Daly and I. I. Negulescu, 'Effect of basic susbtituents on gas sorption and permeation in polysulfone', *Macromolecules*, **29** (1996), 4360–4369.

[165] M. R. Coleman and W. J. Koros, 'Isomeric polyimides based on fluorinated dianhydrides and diamines for gas separation applications', *Journal of Membrane Science*, **50** (1990), 285–297.

[166] T. H. Kim, W. J. Koros, G. R. Husk and K. C. O'Brien, 'Relationship between gas separation properties and chemical structure in a series of aromatic polyimides', *Journal of Membrane Science*, **37** (1988), 45–62.

[167] Y. P. Yampolskii, N. B. Bespalova, E. S. Finkel'shtein, V. Bondar and A. V. Popov, 'Synthesis, gas permeability, and gas sorption properties of fluorine-containing norbornene polymers', *Macromolecules*, **27** (1994), 2872–2878.

[168] R. J. Andrews and E. A. Grulke, 'Glass transition temperatures of polymers, in J. Brandrup, E. H. Immergut, E. A. Grulke, A. Abe and D. R. Bloch (Eds), *Polymer Handbook*, 4th Edn, John Wiley & Sons, Inc., New York, NY, USA (1999), pp. VI 193–VI 278.

[169] V. T. Stannett and M. Szwarc, 'The permeability of polymer films to gases – a simple relationship', *Journal of Polymer Science*, **16** (1955), 89–91.

[170] M. Salame and S. Steingiser, 'Barrier polymers', *Polymer Plastics Technology and Engineering*, **8** (1977), 155–175.

[171] X.-Y. Wang, P. J. in't Veld, Y. Lu, B. D. Freeman and I. C. Sanchez, 'A molecular simulation study of cavity size distributions and diffusion in *para* and *meta* isomers', *Polymer*, **46** (2005), 9155–9161.

[172] A. Morisato, N. R. Mirando, B. D. Freeman and H. B. Hopfenberg, 'The influence of chain configuration and, in turn, chain packing on the sorption and transport properties of poly(*tert* butyl acetylene)', *Journal of Applied Polymer Science*, **49** (1993), 2065–2074.

[173] Y. P. Yampolskii, E. S. Finkelshtein, K. L. Makovetskii, V. Bondar and V. P. Shantarovich, 'Effects of *cis–trans*-configurations of the main chains of poly(trimethylsilyl norbornene) on its transport and sorption properties as well as free volume', *Journal of Applied Polymer Science*, **62** (1996), 349–357.

[174] K. Weh, M. Noack, R. Ruhmann, K. Hoffman, P. Toussaint and J. Caro, 'Modification of the transport properties of a polymethacrylate azobenzene membrane by photochemical switching', *Chemical Engineering Technology*, **21** (1998), 408–412.

[175] P. Zoller and D. J. Walsh, *Standard Pressure–Volume–Temperature Data for Polymers*, Technomic, Lancaster, PA, USA (1995).